Nonlinear $k_\perp$ factorization for quark-gluon dijet production off nuclei

N. N. Nikolaev,[1,2,*] W. Schäfer,[1,†] B. G. Zakharov,[2,‡] and V. R. Zoller[3,§]

[1]*Institut für Kernphysik, Forschungszentrum Jülich, D-52425 Jülich, Germany*
[2]*L. D. Landau Institute for Theoretical Physics, 142432 Chernogolovka, Russia*
[3]*Institute of Theoretical and Experimental Physics, 117259 Moscow, Russia*

(Received 8 April 2005; published 30 August 2005)

The breaking of conventional linear $k_\perp$ factorization for hard processes in a nuclear environment is by now well established. Here we report a detailed derivation of the nonlinear $k_\perp$-factorization relations for the production of quark-gluon dijets. This process is the dominant source of dijets in the proton hemisphere of proton-nucleus collisions at energies of the relativistic heavy ion collider (RHIC). The major technical problem is a consistent description of the non-Abelian intranuclear evolution of multiparton systems of color dipoles. Following the technique developed in our early work [N. N. Nikolaev, W. Schäfer, B. G. Zakharov, and V. R. Zoller, J. Exp. Theor. Phys. **97**, 441 (2003)], we reduce the description of the intranuclear evolution of the $qgg\bar{q}$ state to the 3×3 system of coupled equations in the space of color-singlet 4-parton states $|3\bar{3}\rangle$, $|6\bar{6}\rangle$, and $|1\overline{15}\rangle$ (and their large-N_c generalizations). At large number of colors N_c, the eigenstate $(|6\bar{6}\rangle - |1\overline{15}\rangle)/\sqrt{2}$ decouples from the initial state $|3\bar{3}\rangle$. The resulting nuclear distortions of the dijet spectrum exhibit much similarity to those found earlier for forward dijets in deep inelastic scattering. Still there are certain distinctions regarding the contribution from color-triplet qg final states and from coherent diffraction excitation of dijets. To the large-N_c approximation, we identify four universality classes of nonlinear $k_\perp$ factorization for hard dijet production.

DOI: 10.1103/PhysRevD.72.034033 PACS numbers: 13.87.−a, 11.80.La, 12.38.Bx, 13.85.−t

INTRODUCTION

According to the conventional perturbative QCD (pQCD) factorization theorems the hard scattering cross sections are linear functionals (convolutions) of the appropriate parton densities in the projectile and target [1]. An implicit assumption behind these theorems is that the parton densities in the beam and target are low and the relevant partial wave amplitudes are small, so that the unitarity constraints can be ignored. In the case of hard processes in a nuclear environment, the properly defined partial wave amplitudes become proportional to the nuclear thickness and, for a sufficiently heavy nucleus, overshoot the s-channel unitarity bound. Unitarization makes the nuclear partial waves a highly nonlinear functional of the free-nucleon amplitudes. Alternatively, in the pQCD language, the unitarity constraints bring in a new dimensional scale into the problem—the so-called saturation scale. An important implication of the nonlinear unitarity relation between the free-nucleon and nuclear partial waves is that the properly defined density of gluons in a nucleus becomes a nonlinear functional of the gluon density in a free nucleon; the first discussions of the fusion of partons in deep inelastic scattering (DIS) off a nucleus go back to 1975 [2].

The emergence of a new large scale and the ensuing nonlinearity call for a revision of the pQCD factorization for hard processes in a nuclear environment. A consistent analysis of forward hard dijet production in DIS off nuclei revealed a striking breaking of linear $k_\perp$ factorization [3,4] confirmed later on in the related analysis of single-jet spectra in hadron-nucleus collisions [5,6]. Namely, following the pQCD treatment of diffractive dijet production [7,8], one can define the collective nuclear unintegrated gluon density such that it satisfies the s-channel unitarity constraints and such that the familiar linear $k_\perp$ factorization (see e.g. the recent reviews [9]) would hold for the nuclear structure function $F_{2A}(x, Q^2)$ and the forward single-quark spectrum in DIS off nuclei because of their special Abelian features. However, the dijet spectra in DIS and single-jet spectra in hadron-nucleus collisions prove to be highly nonlinear functionals of the collective nuclear gluon density. Furthermore, the pattern of nonlinearity for single-jet spectra was shown to depend strongly on the relevant partonic subprocess [6]. Our conclusions on the breaking of linear $k_\perp$ factorization for hard scattering off nuclei were recently taken over by other authors [10–12].

In this communication we extend the analysis [4,13] of the excitation of heavy flavor and leading quark dijets in DIS, $\gamma^* g_N \to Q\bar{Q}$, where g_N stands for the gluon exchanged with the nucleon, to the excitation of quark-gluon dijets (pQCD Bremsstrahlung tagged by a scattered quark) in the pQCD subprocess $q^* g_N \to qg$ off free nucleons and its generalization to heavy nuclear targets. In the latter case multiple gluon exchanges between the involved partons and a nucleus are enhanced by a large nuclear radius. The issues are (i) to which extent such multiple gluon exchanges can be described in terms of one and the same unintegrated collective nuclear gluon density and (ii) whether the nuclear factorization for quark-gluon dijets

*Electronic address: N.N.Nikolaev@fz-juelich.de
†Electronic address: Wo.Schaefer@fz-juelich.de
‡Electronic address: B.Zakharov@fz-juelich.de
§Electronic address: zoller@heron.itep.ru

in qA collisions is similar to that for the quark-antiquark dijets in DIS, i.e, in $\gamma^* A$ collisions. To a certain extent, our answer is in the affirmative—the nonlinear $k_\perp$-factorization properties for two processes exhibit much similarity. Still, the two cases differ substantially. For instance, the production of coherent diffractive dijets makes about 50% of the total cross section in DIS but becomes marginal in qA collisions. Furthermore, the contributions from quark-gluon dijets in different color multiplets have very distinct $k_\perp$-factorization properties. Also the effects of the initial-state interaction (ISI) change substantially from the color-singlet γ^* in DIS to the color-triplet quark in qA collisions. On the other hand, the unifying aspect is a treatment of the excitation of final-state color dipoles into the higher color multiplets—color-octet $q\bar{q}$ in DIS and sextet and 15-plet qg in qA collisions. The principal finding from our scrutiny of dijets in DIS and qA collisions and of open charm production in gA collisions is a classification of different nuclear hard processes in four universality classes for nonlinear $k_\perp$ factorization depending on color properties of the pQCD subprocess.

A tempting scenario for hard processes in nuclear matter is hard scattering of the incident parton off the collective nuclear glue preceded and followed by incoherent soft initial and final state interactions. Our consistent S-matrix treatment of the non-Abelian intranuclear evolution of color dipoles is much richer in consequences and such a naive pattern of nuclear factorization is borne out by none of our universality classes: coherent distortions over the whole nucleus or its slices are a common feature of the three universality classes with exception of the open charm production; in the universality class for transition of color dipoles from lower to higher color representations the hard excitation is described by the free-nucleon gluon density; incoherent initial and final state interactions are manifestly absent in the nonlinear $k_\perp$ factorization for the excitation of quark-gluon dijets in the color-triplet state.

The starting point of our analysis is the master formula (13) for the inclusive dijet spectrum. It is derived based on the technique developed in [4,6,14,15] and allows to calculate the dijet spectrum in terms of the S-matrices for interaction with the target nucleon or nucleus of the color-singlet n-parton states, $n = 2, 3, 4$. Within this technique, one deals with infrared-safe quantities despite the fact that the incident parton—the quark q^*—is carrying a net color charge. The calculation of the two-parton and three-parton S-matrices is a single-channel problem with known solution [15–17]. The stumbling block is the calculation of the 4-body S-matrix. In the case of the quark-gluon dijets it describes the non-Abelian intranuclear evolution of the color-singlet $qg\bar{q}g$ system of dipoles. It can be reduced to a 3×3 coupled-channel problem. In our earlier work [4] we published a full solution of the related two-channel problem for the $q\bar{q}q\bar{q}$ system which emerges in the description of quark-antiquark dijets in DIS. Here we report the solution for the $qg\bar{q}g$ system of dipoles which has some new features compared to the $q\bar{q}q\bar{q}$ state in DIS.[1] We go to fine details of this derivation—specifically, the diagonalization of the coupled-channel S-matrix and to the formulation of explicit nonlinear $k_\perp$-factorization formulas for the dijet spectrum—for several reasons. First, the production of quark-gluon dijets without the soft gluon approximation has not been treated before. Second, regarding the color properties of the incident and final states, it is a process of sufficient generality to set a basis for the description of other pQCD processes. In conjunction with our earlier results, it allows to formulate four universality classes of nonlinear $k_\perp$ factorization. Third, recently the formal representation for the dijet cross section similar to our master formula has been discussed by several groups [10–12], but these works stopped short of the diagonalization of their counterpart of our 4-body S-matrix. Correspondingly, they do not contain explicit nonlinear $k_\perp$-factorization formulas.

A very rich pattern of the process-dependent nonlinear $k_\perp$ factorization emerges from the studies presented here and reported in [4,6,13,18]. For instance, it becomes increasingly clear that hard processes in a heavy nucleus cannot be described in terms of a universal collective glue, rather the nuclear glue must be described by a density matrix in the color space. Furthermore, the collective glue defined for a slice of a nucleus rather than the whole nucleus is an indispensable part of the description of excitation of color dipoles into higher color representations, especially in regard to their intranuclear ISI and final-state interaction (FSI) properties. The linear $k_\perp$ factorization for single-quark jets in DIS found in our earlier study [4] is an exception due to the Abelian incident parton—the photon.

From the point of view of practical applications, the discussed quark-gluon dijets are of direct relevance to the large (pseudo)rapidity region of proton-proton and proton-nucleus collisions at RHIC (for the discussion of the possible upgrade of detectors at RHIC II for the improved coverage of the proton fragmentation region see [19]). Our treatment is applicable when the beam and final-state partons interact coherently over the whole longitudinal extension of the nucleus, which at RHIC amounts to the proton fragmentation region of

$$x = \frac{(Q^*)^2 + M_\perp^2}{2mE_{q^*}} \lesssim x_A = \frac{1}{2R_A m_p} \approx 0.1A^{-1/3}, \quad (1)$$

where R_A is the radius of the target nucleus of mass number A, $(Q^*)^2$, and E_{q^*} are the virtuality and energy of the beam quark q^* in the target rest frame, $M_\perp$ is the transverse mass of the dijet and m_p is the proton mass ([2,16], for the

[1] A brief discussion of the main results has been reported elsewhere [18].

related color-dipole phenomenology of the experimental data on nuclear shadowing see [20]).

The presentation of the main material is organized as follows. The master formula for the dijet spectrum is presented in Sec. II. The two-body density matrix—the Fourier transform of which gives the dijet spectrum—contains the S-matrices for the interaction of two-, three-, and four-parton color-singlet systems of dipoles with the target. Based on the technique developed in [15], in Sec. III we report single-channel S-matrices in terms of the quark-antiquark and quark-antiquark-gluon color-dipole cross sections [16,17]. Section IV contains all the technicalities of the derivation of the coupled-channel S-matrix for the $qg\bar{q}g$ state: the decomposition into color multiplets; projection onto the final states; the color-flow diagram technique for the calculation of the 3×3 matrix of color-dipole cross sections; the derivation of the relevant Casimir operators; the explicit diagonalization of the S-matrix at large number of colors N_c, and the Sylvester expansion. The quark-gluon dijet spectrum for the free-nucleon target is derived in Sec. V. Here we also comment on a direct relationship between the dijet and single-jet spectra for the free-nucleon reactions described by the single-gluon exchange in the t-channel. The principal result of this study—the nonlinear $k_\perp$ factorization for the dijet spectrum produced off nuclear targets—is reported in Sec. VI. Here we compare the pattern of nonlinear $k_\perp$ factorization for quark-gluon dijets in qA collisions to that for the quark-antiquark dijets in DIS and gA collisions and identify four universality classes depending on the color representation of the incident parton and final-state dijet. In Sec. VII we apply our results to the nuclear broadening of the dijet acoplanarity distribution. In Sec. VIII we comment on a limiting case when the quark-gluon dijets merge to one jet. Such monojets can be identified with the fragmentation of the quark jet formed by the quasielastically scattered incident quark. The separation into the dijet and monojet final states changes with the mass number of the target nucleus and the centrality of the collisions. We also comment on the possible nuclear modification of the fragmentation function. In the Conclusions section we summarize our main results.

II. THE MASTER FORMULA FOR QUARK-GLUON DIJET PRODUCTION OFF FREE NUCLEONS AND NUCLEI

A. Kinematics and nuclear coherency

To the lowest order in pQCD the underlying subprocess for quark-gluon dijet production in the proton fragmentation region of proton-nucleus collisions is a collision of the valence quark q^* from the proton with the gluon g_N from the target,

$$q^* g_N \to qg.$$

It is a pQCD Bremsstrahlung tagged by a scattered quark. We do not restrict ourselves to radiation of soft gluons. In the case of a nuclear target one has to deal with multiple gluon exchanges which are enhanced by a large thickness of the target nucleus.

From the laboratory, i.e., the nucleus rest frame, standpoint it can be viewed as an excitation of the perturbative $|qg\rangle$ Fock state of the physical projectile $|q^*\rangle$ by one-gluon exchange with the target nucleon or multiple gluon exchanges with the target nucleus. Here the collective nuclear effects develop if the coherency over the thickness of the nucleus holds for the qg Fock states, i.e., if the coherence length is larger than the diameter of the nucleus

$$l_c = \frac{2E_{q^*}}{M_\perp^2 + (Q^*)^2} = \frac{1}{xm_N} > 2R_A, \tag{2}$$

where

$$M_\perp^2 = \frac{\boldsymbol{p}_q^2}{z_q} + \frac{\boldsymbol{p}_g^2}{z_g} \tag{3}$$

is the transverse mass squared of the qg state, $\boldsymbol{p}_{q,g}$ and $z_{q,g}$ are the transverse momenta and fractions of the incident quarks momentum carried by the quark and gluon, respectively, $(z_q + z_g = 1)$.

As a side remark, we note that interactions of the nucleus with the fast beam spectator partons need not be included explicitly, as they would cancel after a proper unitarity sum over spectator final states that is required for the inclusive process in question (see e.g. [6]). The valence quarks of the proton have a small transverse momentum typical of the soft wave function and the interference of radiation of gluons by different valence quarks of the proton is strongly suppressed at large transverse momentum of gluons—notice a close correspondence to the DIS Compton scattering diagram with absorption of the hard photon by one and emission by another quark in the proton which vanishes in the hard regime.

In the antilaboratory (Breit) frame, the partons with the momentum xp_N have a longitudinal localization of the order of their Compton wavelength $\lambda = 1/xp_N$, where p_N is the momentum per nucleon. The coherency over the thickness of the nucleus in the target rest frame is equivalent to the spatial overlap of parton fields of different nucleons at the same impact parameter in the Lorentz-contracted ultrarelativistic nucleus. In the overlap regime one would think of the fusion of partons form different nucleons and collective nuclear parton densities [2]. The overlap takes place if λ exceeds the Lorentz-contracted thickness of the ultrarelativistic nucleus

$$\lambda = \frac{1}{xp_N} > 2R_A \cdot \frac{m_N}{p_N}, \tag{4}$$

which is identical to the condition (2).

Qualitatively, both descriptions of collective nuclear effects are equivalent to each other. Quantitatively, the laboratory frame approach takes advantage of the well-

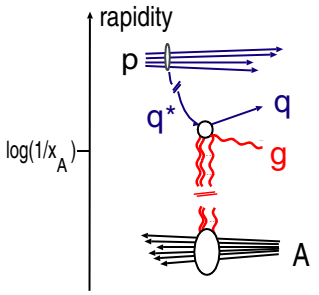

FIG. 1 (color online). The rapidity structure of the radiation of gluons by quarks $q \to qg$ in pA collisions.

developed multiple-scattering theory of interactions of color dipoles with nuclei [4,16,17,21]. From the practical point of view, the coherency condition $x < x_A$ restricts collective effects in hard processes at RHIC to the proton fragmentation region. The target frame rapidity structure of the considered $q^* \to qg$ excitation is shown in Fig. 1. The (pseudo)rapidities of the final-state partons must satisfy $\eta_{q,g} > \eta_A = \log 1/x_A$. The rapidity separation of the quark and gluon hard jets,

$$\Delta\eta_{qg} = \log\frac{1-z_g}{z_g}, \tag{5}$$

is considered to be finite. Both jets are supposed to be separated by a large rapidity from other jets at midrapidity or in the target nucleus hemisphere; the gaps between all jets, beam spectators, and target debris are filled by soft hadrons from an underlying event.

B. Master formula for excitation of quark-gluon dijets

In the nucleus rest frame, relativistic partons q^*, q, and g, propagate along straightline, fixed-impact-parameter, trajectories. To the lowest order in pQCD the Fock state expansion for the physical state $|q^*\rangle_{\rm phys}$ reads

$$|q^*\rangle_{\rm phys} = |q^*\rangle_0 + \Psi(z_g, \boldsymbol{r})|qg\rangle_0, \tag{6}$$

where $\Psi(z_g, \boldsymbol{r})$ is the probability amplitude to find the qg system with the separation $\boldsymbol{r}$ in the two-dimensional impact-parameter space, the subscript "0" refers to bare partons. The perturbative coupling of the $q^* \to qg$ transition is reabsorbed into the light cone wave function $\Psi(z_g, \boldsymbol{r})$. We also omitted a wave function renormalization factor, which is of no relevance for the inelastic excitation to the perturbative order discussed here. The explicit expression for $\Psi(z_g, \boldsymbol{r})$ in terms of the quark-splitting function will be presented below. The wave function depends on the virtuality of the incident q^*, which equals $(Q^*)^2 = (\boldsymbol{p}^*)^2$, where $\boldsymbol{p}^*$ is the transverse momentum of q^* in the incident proton (Fig. 1). For the sake of simplicity we take the collision axis along the momentum of the incident quark q^*, the transformation between the transverse momenta in the q^*-target and p-target reference frames is trivial [6].

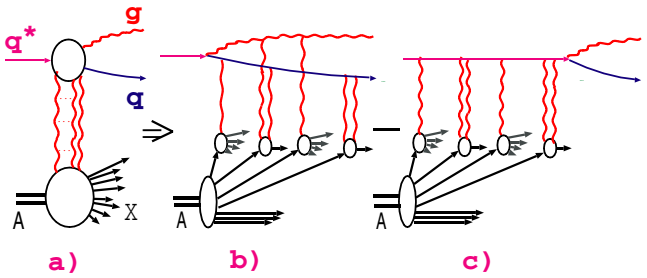

FIG. 2 (color online). Typical contribution to the excitation amplitude for $q^*A \to qgX$, with multiple color excitations of the nucleus. The amplitude receives contributions from processes that involve interactions with the nucleus after and before the virtual decay which interfere destructively.

If $\boldsymbol{b}$ is the impact parameter of the projectile q^*, then the impact parameters of the final-state quark and gluon equal

$$\boldsymbol{b}_q = \boldsymbol{b} - z_g\boldsymbol{r}, \qquad \boldsymbol{b}_g = \boldsymbol{b} + z_q\boldsymbol{r}. \tag{7}$$

By the conservation of impact parameters, the action of the S-matrix on $|a\rangle_{\rm phys}$ takes a simple form

$$\begin{aligned}\mathsf{S}|q^*\rangle_{\rm phys} &= \mathsf{S}_q(\boldsymbol{b})|q^*\rangle_0 + \mathsf{S}_q(\boldsymbol{b}_q)\mathsf{S}_g(\boldsymbol{b}_g)\Psi(z,\boldsymbol{r})|qg\rangle_0 \\ &= \mathsf{S}_q(\boldsymbol{b})|q^*\rangle_{\rm phys} + [\mathsf{S}_q(\boldsymbol{b}_q)\mathsf{S}_g(\boldsymbol{b}_g) \\ &\quad - \mathsf{S}_q(\boldsymbol{b})]\Psi(z_g,\boldsymbol{r})|qg\rangle_0.\end{aligned} \tag{8}$$

In the last line we explicitly decomposed the final state into the (quasi)elastically scattered $|q^*\rangle_{\rm phys}$ and the excited state $|qg\rangle_0$. The two terms in the latter describe a scattering on the target of the qg system formed way in front of the target and the transition $q^* \to qg$ after the interaction of the state $|q^*\rangle_0$ with the target, as illustrated in Fig. 2. The contribution from transitions $q^* \to qg$ inside the target nucleus vanishes in the high-energy limit of $x \lesssim x_A$.[2] We recall, that the s-channel helicity of all partons is conserved.

The probability amplitude for the two-jet spectrum is given by the Fourier transform

$$\begin{aligned}&\int d^2\boldsymbol{b}_q d^2\boldsymbol{b}_g \exp[-i(\boldsymbol{p}_q\boldsymbol{b}_q + \boldsymbol{p}_g\boldsymbol{b}_g)][\mathsf{S}_q(\boldsymbol{b}_q)\mathsf{S}_g(\boldsymbol{b}_g) \\ &\quad - \mathsf{S}_q(\boldsymbol{b})]\Psi(z_g,\boldsymbol{r}).\end{aligned} \tag{9}$$

The differential cross section is proportional to the modulus squared of (9),

[2]In terms of the light cone approach to the QCD Landau-Pomeranchuk-Migdal effect, this corresponds to the thin-target limit [22].

$$\int d^2\boldsymbol{b}'_q d^2\boldsymbol{b}'_g \exp[i(\boldsymbol{p}_q\boldsymbol{b}'_q + \boldsymbol{p}_g\boldsymbol{b}'_g)][\mathsf{S}_q^\dagger(\boldsymbol{b}'_q)\mathsf{S}_g^\dagger(\boldsymbol{b}'_g) - \mathsf{S}_q^\dagger(\boldsymbol{b}')]\Psi^*(z_g,\boldsymbol{r}') \times \int d^2\boldsymbol{b}_q d^2\boldsymbol{b}_g \exp[-i(\boldsymbol{p}_q\boldsymbol{b}_q + \boldsymbol{p}_g\boldsymbol{b}_g)] \times [\mathsf{S}_q(\boldsymbol{b}_q)\mathsf{S}_g(\boldsymbol{b}_g) - \mathsf{S}_q(\boldsymbol{b})]\Psi(z_b,\boldsymbol{r}). \quad (10)$$

The crucial point is that the Hermitian conjugate $\mathsf{S}^\dagger$ can be viewed as the S-matrix for an antiparton [4,14,15]. Consequently, the four terms in the product

$$[\mathsf{S}_q(\boldsymbol{b}'_q)\mathsf{S}_g(\boldsymbol{b}'_g) - \mathsf{S}_q(\boldsymbol{b}')]^\dagger[\mathsf{S}_q(\boldsymbol{b}_q)\mathsf{S}_g(\boldsymbol{b}_g) - \mathsf{S}_q(\boldsymbol{b})]$$

admit a simple interpretation:

$$\mathsf{S}^{(2)}_{q^*q^*}(\boldsymbol{b}',\boldsymbol{b}) = \mathsf{S}_q^\dagger(\boldsymbol{b}')\mathsf{S}_q(\boldsymbol{b}) \quad (11)$$

can be viewed as an S-matrix for elastic scattering on a target of the $\bar{q}^*q^*$ state in which the antiparton $\bar{q}^*$ propagates at the impact parameter $\boldsymbol{b}'$. The averaging over the color states of the beam parton q^* amounts to the dipole $q^*\bar{q}^*$ being in the color-singlet state. Similarly,

$$\begin{aligned}
\mathsf{S}^{(3)}_{\bar{q}^*qg}(\boldsymbol{b}',\boldsymbol{b}_q,\boldsymbol{b}_g) &= \mathsf{S}_q^\dagger(\boldsymbol{b}')\mathsf{S}_q(\boldsymbol{b}_q)\mathsf{S}_g(\boldsymbol{b}_g),\\
\mathsf{S}^{(3)}_{\bar{q}'g'q^*}(\boldsymbol{b},\boldsymbol{b}'_q,\boldsymbol{b}'_g) &= \mathsf{S}_q^\dagger(\boldsymbol{b}'_q)\mathsf{S}_g^\dagger(\boldsymbol{b}'_g)\mathsf{S}_q(\boldsymbol{b}),\\
\mathsf{S}^{(4)}_{\bar{q}'g'gq}(\boldsymbol{b}'_q,\boldsymbol{b}'_g,\boldsymbol{b}_q,\boldsymbol{b}_g) &= \mathsf{S}_q^\dagger(\boldsymbol{b}'_q)\mathsf{S}_g^\dagger(\boldsymbol{b}'_g)\mathsf{S}_g(\boldsymbol{b}_g)\mathsf{S}_q(\boldsymbol{b}_q).
\end{aligned} \quad (12)$$

describe elastic scattering on a target of the overall color-singlet $\bar{q}qg$ and $\bar{q}\,\bar{g}\,gq$ states, respectively. This is shown schematically in Fig. 3. Here we suppressed the matrix elements of $\mathsf{S}^{(n)}$ over the target nucleon, for details of the derivation based on the closure relation, see [4]. Specifically, in the calculation of the inclusive cross sections one averages over the color states of the beam parton q^*, sums over color states X of final-state partons q, g, takes the matrix products of $\mathsf{S}^\dagger$ and S with respect to the relevant color indices entering $\mathsf{S}^{(n)}$ and sums over all nuclear final states applying the closure relation. The technicalities of the derivation of $\mathsf{S}^{(n)}$ will be presented below, here we cite the master formula for the dijet cross section, which is the Fourier transform of the two-body density

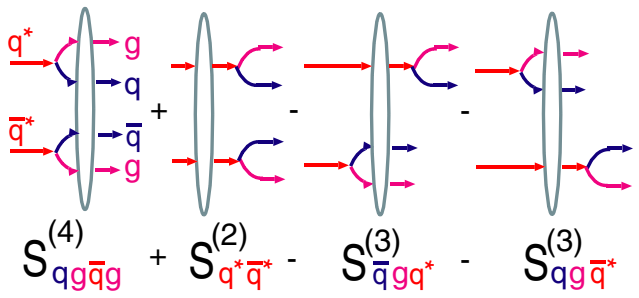

FIG. 3 (color online). The S-matrix structure of the two-body density matrix for excitation $q^* \to qg$.

matrix:

$$\begin{aligned}
\frac{d\sigma(q^* \to qg)}{dz d^2\boldsymbol{p}_q d^2\boldsymbol{p}_g} = \frac{1}{(2\pi)^4}\int d^2\boldsymbol{b}_q d^2\boldsymbol{b}_g d^2\boldsymbol{b}'_q d^2\boldsymbol{b}'_g \\
\times \exp[-i\boldsymbol{p}_q(\boldsymbol{b}_q - \boldsymbol{b}'_q) - i\boldsymbol{p}_g(\boldsymbol{b}_g - \boldsymbol{b}'_g)] \\
\times \Psi(z_g,\boldsymbol{b}_q - \boldsymbol{b}_g)\Psi^*(z_g,\boldsymbol{b}'_q - \boldsymbol{b}'_g) \\
\times \sum_X \langle X|\{\mathsf{S}^{(4)}_{\bar{q}g'qg}(\boldsymbol{b}'_q,\boldsymbol{b}'_g,\boldsymbol{b}_q,\boldsymbol{b}_g) \\
+ \mathsf{S}^{(2)}_{\bar{q}^*q^*}(\boldsymbol{b}',\boldsymbol{b}) - \mathsf{S}^{(3)}_{\bar{q}g'q^*}(\boldsymbol{b},\boldsymbol{b}'_q,\boldsymbol{b}'_g) \\
- \mathsf{S}^{(3)}_{\bar{q}^*qg}(\boldsymbol{b}',\boldsymbol{b}_q,\boldsymbol{b}_g)\}|\mathrm{in}\rangle.
\end{aligned} \quad (13)$$

Hereafter, we describe the final-state dijet in terms of the gluon-jet momentum, $\boldsymbol{p} \equiv \boldsymbol{p}_g$, $z \equiv z_g$, and the decorrelation (acoplanarity) momentum $\Delta = \boldsymbol{p}_q + \boldsymbol{p}_g$. We also introduce

$$\boldsymbol{s} = \boldsymbol{b}_q - \boldsymbol{b}'_q, \quad (14)$$

in terms of which $\boldsymbol{b}_g - \boldsymbol{b}'_g = \boldsymbol{s} + \boldsymbol{r} - \boldsymbol{r}'$ and

$$\begin{aligned}
&\exp[-i\boldsymbol{p}_q(\boldsymbol{b}_q - \boldsymbol{b}'_q) - i\boldsymbol{p}_q(\boldsymbol{b}_g - \boldsymbol{b}'_g)] \\
&\quad = \exp[-i\Delta\boldsymbol{s} - i\boldsymbol{p}\boldsymbol{r} + i\boldsymbol{p}\boldsymbol{r}'],
\end{aligned} \quad (15)$$

so that the dipole parameter $\boldsymbol{s}$ is conjugate to the acoplanarity momentum Δ.

III. CALCULATION OF THE 2-PARTON AND 3-PARTON S-MATRICES

A. The quark-nucleon S-matrix and the $k_\perp$-factorization representations for the color-dipole cross section

In order to set up the formalism, we start with the S-matrix representation for the cross section of interaction of the triplet-antitriplet color dipole $q\bar{q}$ with the free-nucleon target [4]. To the two-gluon exchange approximation, the S-matrices of the quark-nucleon and antiquark-nucleon interaction at an impact parameter $\boldsymbol{b}_q(\boldsymbol{b}_{\bar{q}})$ equal, respectively,

$$\begin{aligned}
\mathsf{S}(\boldsymbol{b}_q) &= 1 + iT^aV_a\chi(\boldsymbol{b}_q) - \frac{1}{2}T^aT^a\chi^2(\boldsymbol{b}_q),\\
\mathsf{S}^\dagger(\boldsymbol{b}_{\bar{q}}) &= 1 - iT^aV_a\chi(\boldsymbol{b}_{\bar{q}}) - \frac{1}{2}T^aT^a\chi^2(\boldsymbol{b}_{\bar{q}}),
\end{aligned} \quad (16)$$

where $T^aV_a\chi(\boldsymbol{b})$ is the eikonal for the quark-nucleon gluon exchange. The vertex V_a for excitation of the nucleon $g^aN \to N^*_a$ into color-octet state is so normalized that after application of closure over the final-state excitations N^* the vertex g^ag^bNN equals $\langle N|V_a^\dagger V_b|N\rangle = \delta_{ab}$. The second order terms in (16) do already use this normalization. The S-matrix of the $(q\bar{q})$-nucleon interaction equals

$$\mathsf{S}^{(2)}_{q\bar{q}}(\boldsymbol{b}_q,\boldsymbol{b}_{\bar{q}}) = \frac{\langle N|\mathrm{Tr}[\mathsf{S}(\boldsymbol{b}_q)\mathsf{S}^\dagger(\boldsymbol{b}_{\bar{q}})]|N\rangle}{\langle N|\mathbb{1}|N\rangle\mathrm{Tr}\mathbb{1}}. \quad (17)$$

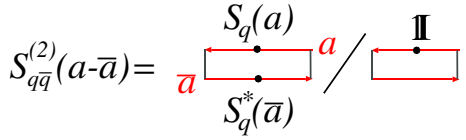

FIG. 4 (color online). The color-flow diagram for the S-matrix for the interaction of the color-single $q\bar{q}$ dipole with the nucleon; a and $\bar{a}$ are the impact parameters of the quark and antiquark, respectively.

A graphical rule for the calculation of the color traces entering (17) is shown in Fig. 4; such color-flow diagrams will extensively be used in the subsequent calculation of $\mathsf{S}^{(4)}$.

The corresponding profile function is $\Gamma_2(\boldsymbol{b}_q, \boldsymbol{b}_{\bar{q}}) = 1 - \mathsf{S}^{(2)}_{q\bar{q}}(\boldsymbol{b}_q, \boldsymbol{b}_{\bar{q}})$. The dipole cross section for interaction of the color-singlet $q\bar{q}$ dipole $\boldsymbol{r} = \boldsymbol{b}_q - \boldsymbol{b}_{\bar{q}}$ with the free nucleon is obtained upon the integration over the overall impact parameter

$$\sigma(\boldsymbol{r}) = 2\int d^2\boldsymbol{b}_q \Gamma_2(\boldsymbol{b}_q, \boldsymbol{b}_q - \boldsymbol{r}) = C_F \int d^2\boldsymbol{b}_q [\chi(\boldsymbol{b}_q) - \chi(\boldsymbol{b}_q - \boldsymbol{r})]^2, \quad (18)$$

where $C_F = (N_c^2 - 1)/2N_c$ is the quark Casimir operator. It sums a contribution from the four Feynman diagrams of Fig. 5 and is related to the gluon density in the target by the $k_\perp$-factorization formula [17,23]

$$\sigma(x, \boldsymbol{r}) = \int d^2\boldsymbol{\kappa} f(x, \boldsymbol{\kappa})[1 - \exp(i\boldsymbol{\kappa}\boldsymbol{r})], \quad (19)$$

where

$$f(x, \boldsymbol{\kappa}) = \frac{4\pi\alpha_S(r)}{N_c} \cdot \frac{1}{\kappa^4} \cdot \mathcal{F}(x, \kappa^2) \quad (20)$$

and

$$\mathcal{F}(x, \kappa^2) = \frac{\partial G(x, \kappa^2)}{\partial \log \kappa^2} \quad (21)$$

is the unintegrated gluon density in the target nucleon. Hereafter, unless it may cause a confusion, we suppress the variable x in the gluon densities and dipole cross sections. The leading $\mathrm{Log}\frac{1}{x}$ evolution of the dipole cross section is governed by the color-dipole leading-$\mathrm{Log}\frac{1}{x}$ evolution [17,24], the same evolution for the unintegrated gluon density is governed by the familiar momentum-space Balitskii-Fadin-Kuraev-Lipatov (BFKL) equation [25].

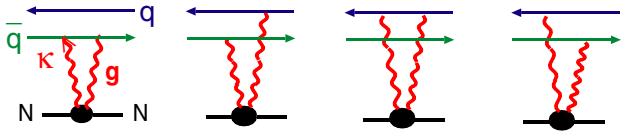

FIG. 5 (color online). The four Feynman diagrams for the quark-antiquark dipole-nucleon interaction by the two-gluon pomeron exchange in the t-channel.

The S-matrix for coherent interaction of the color dipole with the nuclear target is given by the Glauber-Gribov formula [26,27]

$$\mathsf{S}[\boldsymbol{b}, \sigma(\boldsymbol{r})] = \exp\left[-\frac{1}{2}\sigma(\boldsymbol{r})T(\boldsymbol{b})\right], \quad (22)$$

where

$$T(\boldsymbol{b}) = \int_{-\infty}^{\infty} dr_z n_A(\boldsymbol{b}, r_z) \quad (23)$$

is the optical thickness of the nucleus. The nuclear density $n_A(\boldsymbol{b}, r_z)$ is normalized according to $\int d^3\vec{r} n_A(\boldsymbol{b}, r_z) = \int d^2\boldsymbol{b} T(\boldsymbol{b}) = A$, where A is the nuclear mass number.

In the specific case of $\mathsf{S}^{(2)}_{q^*q^*}(\boldsymbol{b}', \boldsymbol{b})$ the color dipole equals

$$\boldsymbol{r}_{q\bar{q}} = \boldsymbol{b} - \boldsymbol{b}' = \boldsymbol{s} + z\boldsymbol{r} - z\boldsymbol{r}' \quad (24)$$

and $\mathsf{S}^{(2)}_{\bar{q}^*q^*}(\boldsymbol{b}', \boldsymbol{b})$ entering Eq. (14) will be given by the Glauber-Gribov formula

$$\mathsf{S}^{(2)}_{\bar{q}^*q^*}(\boldsymbol{b}', \boldsymbol{b}) = S[\boldsymbol{b}, \sigma(\boldsymbol{s} + z\boldsymbol{r} - z\boldsymbol{r}')]. \quad (25)$$

B. The S-matrix for the color-singlet $\bar{q}qg$ state

Here quark and gluon couple to the color triplet. The dipole cross section for the color-singlet $\bar{q}qg$ state has been derived in [17], the S-matrix derivation with the quark-antiquark basis description of the gluon is found in Appendix A of Ref. [6]. For the generic 3-body state shown in Fig. 6 it equals

$$\sigma_3(\boldsymbol{r}_{q\bar{q}}, \boldsymbol{r}_{gq}) = \frac{C_A}{2C_F}[\sigma(\boldsymbol{r}_{gq}) + \sigma(\boldsymbol{r}_{g\bar{q}}) - \sigma(\boldsymbol{r}_{q\bar{q}})] + \sigma(\boldsymbol{r}_{q\bar{q}}), \quad (26)$$

where $\boldsymbol{r}_{g\bar{q}} = \boldsymbol{r}_{gq} + \boldsymbol{r}_{q\bar{q}}$. The configuration of color dipoles for the case of our interest is shown in Fig. 6 (see the related derivation in [15]). For the $\bar{q}^*qg$ state the relevant

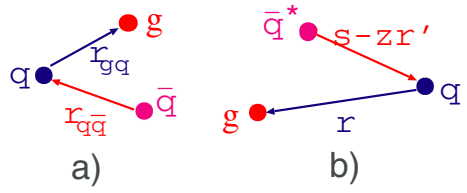

FIG. 6 (color online). The color-dipole structure of (a) the generic quark-antiquark-gluon system of dipoles and (b) of the $\bar{q}^*qg$ system which emerges in the S-matrix structure of the two-body density matrix for excitation $q^* \to qg$.

dipole sizes in (26) equal

$$\begin{aligned} \boldsymbol{r}_{q\bar{q}} &= \boldsymbol{b}_q - \boldsymbol{b}' = \boldsymbol{s} - z\boldsymbol{r}, \qquad \boldsymbol{r}_{gq} = \boldsymbol{b}_g - \boldsymbol{b}_q = \boldsymbol{r}, \\ \boldsymbol{r}_{g\bar{q}} &= \boldsymbol{b}_g - \boldsymbol{b}' = \boldsymbol{s} + \boldsymbol{r} - z\boldsymbol{r}', \end{aligned} \tag{27}$$

whereas for the $q^*\bar{q}g'$ state we have

$$\begin{aligned} \boldsymbol{r}_{q\bar{q}} &= \boldsymbol{b} - \boldsymbol{b}'_q = \boldsymbol{s} + z\boldsymbol{r}, \qquad \boldsymbol{r}_{gq} = \boldsymbol{b}'_g - \boldsymbol{b}'_q = \boldsymbol{r}', \\ \boldsymbol{r}_{g\bar{q}} &= \boldsymbol{b}_g - \boldsymbol{b} = \boldsymbol{s} + z\boldsymbol{r} - \boldsymbol{r}', \end{aligned} \tag{28}$$

so that

$$\begin{aligned} \sigma_{\bar{q}^* qg} &= \frac{C_A}{2C_F}[\sigma(\boldsymbol{r}) + \sigma(\boldsymbol{s} + \boldsymbol{r} - z\boldsymbol{r}') - \sigma(\boldsymbol{s} - z\boldsymbol{r}')] \\ &\quad + \sigma(\boldsymbol{s} - z\boldsymbol{r}'), \\ \sigma_{q^*\bar{q}'g'} &= \frac{C_A}{2C_F}[\sigma(-\boldsymbol{r}') + \sigma(\boldsymbol{s} - \boldsymbol{r}' + z\boldsymbol{r}) - \sigma(\boldsymbol{s} + z\boldsymbol{r})] \\ &\quad + \sigma(\boldsymbol{s} + z\boldsymbol{r}). \end{aligned} \tag{29}$$

The overall color-singlet $q\bar{q}g$ state has a unique color structure and its elastic scattering on a nucleus is a single-channel problem. Consequently, the nuclear S-matrix is given by the single-channel Glauber-Gribov formula [26,27]

$$\begin{aligned} \mathsf{S}^{(3)}_{\bar{q}'g'q^*}(\boldsymbol{b}, \boldsymbol{b}'_q, \boldsymbol{b}'_g) &= \mathsf{S}[\boldsymbol{b}, \sigma_{q^*\bar{q}'g'}], \\ \mathsf{S}^{(3)}_{\bar{q}^* qg}(\boldsymbol{b}', \boldsymbol{b}_q, \boldsymbol{b}_g) &= \mathsf{S}[\boldsymbol{b}, \sigma_{\bar{q}^* qg}]. \end{aligned} \tag{30}$$

IV. COUPLED-CHANNEL S-MATRIX FOR THE 4-PARTON STATE

A. The basis of color-singlet ($q\bar{q}gg'$) states

The 4-parton S-matrix describes transitions between color-singlet ($q\bar{q}gg'$) states. It is convenient to decompose the $|qg\rangle$ state into the $|3\rangle$, $|6\rangle$, and $|15\rangle$ states and their $SU(N_c)$ generalizations (our reference to the triplet, sextet, and 15-plet states at arbitrary N_c should not cause any confusion). Then the basis of color-singlet states $|q\bar{q}gg'\rangle$ will consist of the $|3\bar{3}\rangle$, $|6\bar{6}\rangle$, and $|15\overline{15}\rangle$ systems of color dipoles and the intranuclear evolution in the elastic scattering of the 4-parton state off the nucleus is a three-channel problem. The evolution starts from the $|3\bar{3}\rangle$ state what is evident from Fig. 3. Technically, once the 3×3 matrix $\hat{\Sigma}$ of 4-body dipole cross sections is known, the corresponding nuclear S-matrix will be given by the Glauber-Gribov formula

$$\mathsf{S}^{(4)}_{\bar{q}'g'gq}(\boldsymbol{b}'_q, \boldsymbol{b}'_g, \boldsymbol{b}_q, \boldsymbol{b}_g) = \mathsf{S}[\boldsymbol{b}, \hat{\Sigma}]. \tag{31}$$

Our immediate task is a calculation of the coupled-channel operator $\hat{\Sigma}$.

We chose a description of the gluon in the quark-antiquark basis:

$$g^i_k = \bar{a}^i a_k - \frac{1}{N_c}(\bar{a}a)\delta^i_k. \tag{32}$$

In the calculation of the S-matrices both the quark a and the antiquark $\bar{a}$ must be considered as propagating at the same impact parameter. The generic quark-gluon state is described by a tensor

$$v^i_{kl} = g^i_k c_l = \bar{a}^i a_k c_l - \frac{1}{N_c}(\bar{a}a)c_l\delta^i_k. \tag{33}$$

There is a unique color-triplet quark-gluon state (the normalization of the states will be defined at the level of the $|3\bar{3}\rangle$, $|6\bar{6}\rangle$, and $|15\overline{15}\rangle$ systems of color dipoles)

$$t_k = (\bar{a}c)a_k - \frac{1}{N_c}(\bar{a}a)c_k. \tag{34}$$

The sextet state is described by the traceless tensor antisymmetric in (k, l),

$$\begin{aligned} A^i_{kl} &= \bar{a}^i(a_k c_l - a_l c_k) + \frac{1}{N_c - 1}[(\bar{a}c)a_l - (\bar{a}a)c_l]\delta^i_k \\ &\quad - \frac{1}{N_c - 1}[(\bar{a}c)a_k - (\bar{a}a)c_k]\delta^i_l, \end{aligned} \tag{35}$$

while the 15-plet is described by the traceless symmetric tensor

$$\begin{aligned} S^i_{kl} &= \bar{a}^i(a_k c_l + a_l c_k) - \frac{1}{N_c + 1}[(\bar{a}c)a_l + (\bar{a}a)c_l]\delta^i_k \\ &\quad - \frac{1}{N_c + 1}[(\bar{a}c)a_k + (\bar{a}a)c_k]\delta^i_l. \end{aligned} \tag{36}$$

The quark, antiquark, and two gluons in the color-singlet ($q\bar{q}gg'$) system of dipoles all propagate at different impact parameters. To avoid confusion, the gluon in the complex conjugated state will be described by the tensor

$$(g')^i_k = \bar{b}^i b_k - \frac{1}{N_c}(\bar{b}b)\delta^i_k, \tag{37}$$

and the antitriplet state is

$$\bar{t}^k = (\bar{c}b)\bar{b}^k - \frac{1}{N_c}(\bar{b}b)\bar{c}^k. \tag{38}$$

The overall color-singlet $|3\bar{3}\rangle$, $|6\bar{6}\rangle$, and $|15\overline{15}\rangle$ states will be decomposed into six 6-body color-singlet states. The corresponding 6-body vertices (projection operators) equal

$$\begin{aligned} V_1 &= (\bar{a}b)(\bar{b}a)(\bar{c}c), \qquad V_2 = (\bar{a}b)(\bar{b}c)(\bar{c}a), \\ V_3 &= (\bar{a}a)(\bar{b}c)(\bar{c}b), \qquad V_4 = (\bar{a}c)(\bar{b}b)(\bar{c}a), \\ V_5 &= (\bar{a}c)(\bar{b}a)(\bar{c}b), \qquad V_6 = (\bar{a}a)(\bar{b}b)(\bar{c}c), \end{aligned} \tag{39}$$

some of which are pictorially represented in Fig. 7. For instance, the normalized color-singlet triplet-antitriplet state will be

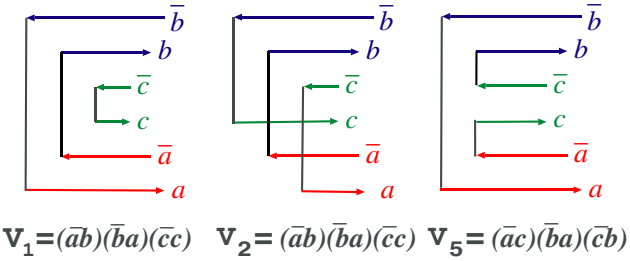

FIG. 7 (color online). Examples of the 6-body vertices (projection operators) which emerge in expansions of the $qg\bar{q}g$ states in the quark-antiquark basis.

$$|3\bar{3}\rangle = \left[-\frac{1}{N_c}V_3 - \frac{1}{N_c}V_4 + V_5 + \frac{1}{N_c^2}V_6\right]\cdot\frac{\sqrt{N_c}}{(N_c^2-1)}. \tag{40}$$

Similarly, one finds

$$|6\bar{6}\rangle = \left[V_1 - V_2 + \frac{1}{N_c-1}(V_3 + V_4 - V_5 - V_6)\right] \times \frac{1}{\sqrt{2N_c(N_c+1)(N_c-2)}}, \tag{41}$$

$$|15\overline{15}\rangle = \left[V_1 + V_2 - \frac{1}{N_c+1}(V_3 + V_4 + V_5 + V_6)\right] \times \frac{1}{\sqrt{2N_c(N_c-1)(N_c+2)}}. \tag{42}$$

These states are normalized to unity, $\langle 3\bar{3}|3\bar{3}\rangle = \langle 6\bar{6}|6\bar{6}\rangle = \langle 15\overline{15}|15\overline{15}\rangle = 1$, the normalization coefficients are readily derived using the color-flow diagram technique described in Sec. IV C below. The diagonal and off-diagonal matrix elements of the 4-body cross section operator in the basis of $|3\bar{3}\rangle$, $|6\bar{6}\rangle$, and $|15\overline{15}\rangle$ of color-dipole states will be decomposed in terms of the matrix elements

$$\sigma_{ik} = \langle V_i|\hat{\Sigma}|V_k\rangle \tag{43}$$

with the coefficients given by the expansions (40)–(42).

Note that each of the σ_{ik} is a matrix element between the overall color-singlet 6-body configurations composed of the three color-singlet quark-antiquark pairs. As such all of them are infrared-safe quantities.

B. Projection onto the final states

In the case of the inclusive dijet spectrum with summation over all colors of final-state quarks and gluons the projection onto the final state is of the form (see the discussion in [4])

$$\sum_X \langle X| = \sum_R \sqrt{\dim(R)}\langle R\bar{R}| = \sqrt{N_c}\langle 3\bar{3}| + \sqrt{\frac{1}{2}N_c(N_c+1)(N_c-2)}\langle 6\bar{6}| + \sqrt{\frac{1}{2}N_c(N_c-1)(N_c+2)}\langle 15\overline{15}|, \tag{44}$$

where $\dim(R)$ is the dimension of the corresponding representation. The averaging over the colors of the initial quark q^* amounts to taking

$$|\mathrm{in}\rangle = |3\bar{3}\rangle\cdot\frac{1}{\sqrt{\dim(3)}}. \tag{45}$$

Then the calculation of the inclusive dijet cross section requires the evaluation of the combination of matrix elements

$$\sum_X \langle X|\mathsf{S}[\boldsymbol{b},\hat{\Sigma}]|\mathrm{in}\rangle = \langle 3\bar{3}|\mathsf{S}[\boldsymbol{b},\hat{\Sigma}]|3\bar{3}\rangle + \sqrt{\frac{\dim(6)}{\dim(3)}}\langle 6\bar{6}|\mathsf{S}[\boldsymbol{b},\hat{\Sigma}]|3\bar{3}\rangle + \sqrt{\frac{\dim(15)}{\dim(3)}}\langle 15\overline{15}|\mathsf{S}[\boldsymbol{b},\hat{\Sigma}]|3\bar{3}\rangle. \tag{46}$$

Besides the inclusive spectrum one can readily consider the excitation of quark-gluon dijets in specific color representations. We reiterate that they also will be infrared-safe observables.

C. Color-flow diagrams

The calculation of the matrix elements (43) is greatly simplified by the technique of color-flow diagrams. Each matrix element (43) corresponds to a certain color-flow diagram. Altogether there are 21 different color-flow diagrams, the three selected cases are shown in Fig. 8. The number of closed loops varies from three to one. In the calculation of the S-matrix elements,

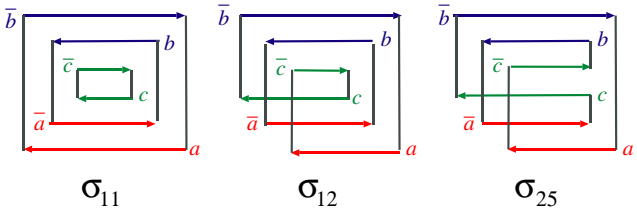

FIG. 8 (color online). Examples of color-flow diagrams for the calculation of the components of the 6-body dipole cross sections. The horizontal quark lines are multiplied by the quark S-matrix $\mathsf{S}(\boldsymbol{b}_i)$ taken at the appropriate impact parameter, while each horizontal antiquark line is multiplied by $\mathsf{S}^\dagger(\boldsymbol{b}_i)$, the trace is taken for each closed loop.

$$\mathsf{S}_{ik} = \langle V_i|\mathsf{S}|V_k\rangle, \tag{47}$$

each horizontal quark line is multiplied by the quark S-matrix $\mathsf{S}(\boldsymbol{b}_i)$ taken at the appropriate impact parameter $\boldsymbol{b}_i$, while the antiquark line is multiplied by $\mathsf{S}^\dagger(\boldsymbol{b}_i)$. The trace of the product of S-matrices is calculated for each closed loop.

The first application of the color-flow diagrams is to the derivation of the normalization factors in expansions (41). They are obtained by assigning the factor N_c to each and every loop.

Now we present the results for the three matrix elements shown in Fig. 8. For the sake of brevity the impact parameters of quarks and antiquarks will be denoted by their symbols. One readily finds

$$\begin{aligned}\mathsf{S}_{11} &= \langle V_1|\mathsf{S}|V_1\rangle \\ &= \mathrm{Tr}[\mathsf{S}(a)\mathsf{S}^\dagger(\bar b)]\mathrm{Tr}[\mathsf{S}(b)\mathsf{S}^\dagger(\bar a)]\mathrm{Tr}[\mathsf{S}(c)\mathsf{S}^\dagger(\bar c)] \\ &= N_c^3[1-\Gamma(a-\bar b)][1-\Gamma(b-\bar a)][1-\Gamma(c-\bar c)].\end{aligned} \tag{48}$$

The multibody S-matrices must be evaluated up to the terms quadratic in the QCD eikonal, i.e., to the terms linear in the triplet-antitritplet color-dipole profile function Γ, and the corresponding matrix element of the dipole cross section equals

$$\begin{aligned}\sigma_{11} &= \langle V_1|\hat\Sigma|V_1\rangle \\ &= N_c^3[\sigma(a-\bar b)+\sigma(b-\bar a)+\sigma(c-\bar c)] \\ &= N_c^3[2\sigma(a-b)+\sigma(c-\bar c)].\end{aligned} \tag{49}$$

Each quark-antiquark loop gives the corresponding dipole cross section times N_c to the power equal to the number of loops. Here we took into account that the quark a and antiquark $\bar a$, and b and $\bar b$ as well, propagate pairwise at equal impact parameters.

The case of σ_{12} is a bit more complicated. Here S_{12} is a product of two traces:

$$\begin{aligned}\mathsf{S}_{12} &= \langle V_1|\mathsf{S}|V_2\rangle \\ &= \mathrm{Tr}[\mathsf{S}(b)\mathsf{S}^\dagger(\bar a)]\mathrm{Tr}[\mathsf{S}(a)\mathsf{S}^\dagger(\bar b)\mathsf{S}(c)\mathsf{S}^\dagger(\bar c)] \\ &= N_c[1-\Gamma(b-\bar a)]\mathrm{Tr}[\mathsf{S}(a)\mathsf{S}^\dagger(\bar b)\mathsf{S}(c)\mathsf{S}^\dagger(\bar c)].\end{aligned} \tag{50}$$

The latter trace $\mathrm{Tr}[\mathsf{S}(a)\mathsf{S}^\dagger(\bar b)\mathsf{S}(c)\mathsf{S}^\dagger(\bar c)]$ was already encountered in our derivation of the 4-parton S-matrix for the production of dijets in DIS [4]. The corresponding color-flow diagram is shown in Fig. 9. Here one needs to sum the contributions to the $\bar b c\bar c a$ scattering amplitude from the exchange by the 2-gluon pomerons in the t-channel. The familiar diagram of Fig. 9(a) gives a contribution $-\chi(c)\chi(\bar c)\mathrm{Tr}(\mathsf{T}^a\mathsf{T}^a)$. The new case is when the

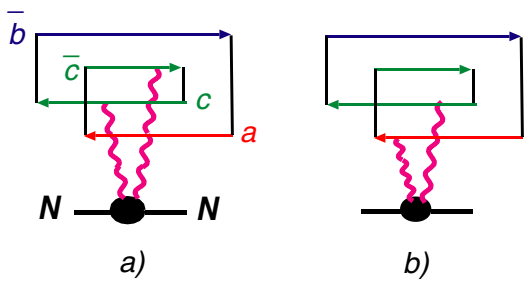

FIG. 9 (color online). Examples of interaction with the target nucleon of the (a) quark-antiquark and diquark dipole in the $\bar b c\bar c a$ state.

two gluons are attached to the diquark ac as shown in Fig. 9(b). Straightforward algebra shows that the corresponding contribution to the profile function equals $\chi(a)\chi(c)\mathrm{Tr}(\mathsf{T}^a\mathsf{T}^a)$. This gives rise to a simple rule: each quark-antiquark pair, $a\bar b$, $a\bar c$, $c\bar b$, and $c\bar c$, contributes the corresponding triplet-antitriplet dipole cross section, whereas the diquark ac and the antidiquark $\bar b\,\bar c$ contribute the triplet-antitriplet dipole cross section taken with the negative sign. The color traces give a factor N_c per each loop, one of these factors has already been put in evidence in Eq. (50). The final result is

$$\begin{aligned}\sigma_{12} &= \langle V_1|\hat\Sigma|V_2\rangle \\ &= N_c^2[\sigma(b-\bar a)+\sigma(a-\bar b)-\sigma(a-c)+\sigma(a-\bar c) \\ &\quad +\sigma(c-\bar b)-\sigma(\bar b-\bar c)+\sigma(c-\bar c)].\end{aligned} \tag{51}$$

Application of the same technique to σ_{25} gives

$$\begin{aligned}\mathsf{S}_{25} &= \langle V_2|\mathsf{S}|V_5\rangle \\ &= \mathrm{Tr}[\mathsf{S}(a)\mathsf{S}^\dagger(\bar a)\mathsf{S}^\dagger(\bar c)\mathsf{S}(b)\mathsf{S}^\dagger(\bar a)\mathsf{S}(c)\mathsf{S}^\dagger(\bar b)]\end{aligned} \tag{52}$$

with the cross section

$$\begin{aligned}\sigma_{25} &= \langle V_2|\hat\Sigma|V_5\rangle \\ &= N_c[\sigma(a-\bar c)-\sigma(a-b)+\sigma(a-\bar a)-\sigma(a-c) \\ &\quad +\sigma(a-\bar b)+\sigma(b-\bar c)-\sigma(\bar a-\bar c)+\sigma(c-\bar c) \\ &\quad -\sigma(\bar c-\bar b)+\sigma(b-\bar a)-\sigma(b-c)+\sigma(b-\bar b) \\ &\quad +\sigma(c-\bar a)-\sigma(\bar a-\bar b)+\sigma(c-\bar b)] \\ &= N_c\sigma(c-\bar c)\end{aligned} \tag{53}$$

Here we used the obvious properties $\sigma(a-\bar a)=\sigma(b-\bar b)=0$ and cancellations due to equalities of the form $\sigma(c-a)=\sigma(c-\bar a)$. For the sake of completeness, we cite all the remaining σ_{ik}:

$$\sigma_{13} = N_c\sigma(c-\bar{c}), \qquad \sigma_{14} = N_c\sigma(c-\bar{c}),$$
$$\sigma_{15} = N_c^2[2\sigma(a-b)+\sigma(c-\bar{c})+\sigma(a-c)+\sigma(b-c)-\sigma(b-c)-\sigma(a-\bar{c})], \qquad \sigma_{16} = N_c^2\sigma(c-\bar{c}),$$
$$\sigma_{22} = N_c^3[\sigma(a-b)+\sigma(b-c)+\sigma(a-\bar{c})], \qquad \sigma_{23} = N_c^2[\sigma(b-c)+\sigma(b-\bar{c})],$$
$$\sigma_{24} = N_c^2[\sigma(a-c)+\sigma(a-\bar{c})], \qquad \sigma_{26} = N_c\sigma(c-\bar{c}), \qquad \sigma_{33} = N_c^3[\sigma(b-c)+\sigma(b-\bar{c})], \tag{54}$$
$$\sigma_{34} = N_c\sigma(c-\bar{c}), \qquad \sigma_{35} = N_c^2[\sigma(b-c)+\sigma(b-\bar{c})], \qquad \sigma_{36} = N_c^2\sigma(c-\bar{c}),$$
$$\sigma_{44} = N_c^3[\sigma(a-c)+\sigma(a-\bar{c})], \qquad \sigma_{45} = N_c^2[\sigma(a-c)+\sigma(a-\bar{c})], \qquad \sigma_{46} = N_c^2\sigma(c-\bar{c}),$$
$$\sigma_{55} = N_c^3[\sigma(a-b)+\sigma(a-c)+\sigma(b-\bar{c})], \qquad \sigma_{56} = N_c\sigma(c-\bar{c}), \qquad \sigma_{66} = N_c^3\sigma(c-\bar{c}).$$

D. The 3×3 matrix of 4-parton dipole cross sections $\hat{\Sigma}$.

A simple algebra gives the following 3×3 matrix $\hat{\Sigma}$ of 4-body dipole cross sections (we go back to the dipole parameters defined in Sec. II):

$$\Sigma_{11} = \langle 3\bar{3}|\hat{\Sigma}|3\bar{3}\rangle = \frac{C_A}{2C_F}[\sigma(\boldsymbol{s}-\boldsymbol{r}'+\boldsymbol{r})+\sigma(\boldsymbol{r})+\sigma(\boldsymbol{r}')] - \frac{1}{N_c^2-1}\sigma(\boldsymbol{s}) - \frac{C_A}{2C_F}\cdot\frac{1}{N_c^2-1}\Omega, \tag{55}$$

where

$$\Omega = \sigma(\boldsymbol{s}-\boldsymbol{r}')+\sigma(\boldsymbol{s}+\boldsymbol{r})-\sigma(\boldsymbol{s}-\boldsymbol{r}'+\boldsymbol{r})-\sigma(\boldsymbol{s}). \tag{56}$$

Similar calculation gives

$$\Sigma_{22} = \langle 6\bar{6}|\hat{\Sigma}|6\bar{6}\rangle = \frac{3N_c+1}{N_c+1}\cdot\frac{1}{2}\cdot[\sigma(\boldsymbol{s}-\boldsymbol{r}'+\boldsymbol{r})+\sigma(\boldsymbol{s})] + \frac{N_c^2+1}{2(N_c^2-1)}\cdot[\sigma(\boldsymbol{s}-\boldsymbol{r}'+\boldsymbol{r})-\sigma(\boldsymbol{s})] + \frac{N_c}{N_c^2-1}[\sigma(\boldsymbol{r})+\sigma(\boldsymbol{r}')] - \frac{N_c}{2(N_c+1)}\cdot\left[1+\frac{1}{(N_c-1)^2}\right]\Omega, \tag{57}$$

$$\Sigma_{33} = \langle 15\overline{15}|\hat{\Sigma}|15\overline{15}\rangle = \frac{3N_c-1}{N_c-1}\cdot\frac{1}{2}\cdot[\sigma(\boldsymbol{s}-\boldsymbol{r}'+\boldsymbol{r})+\sigma(\boldsymbol{s})] + \frac{N_c^2+1}{2(N_c^2-1)}\cdot[\sigma(\boldsymbol{s}-\boldsymbol{r}'+\boldsymbol{r})-\sigma(\boldsymbol{s})] - \frac{N_c}{N_c^2-1}[\sigma(\boldsymbol{r})+\sigma(\boldsymbol{r}')] - \frac{N_c}{2(N_c-1)}\cdot\left[1+\frac{1}{(N_c+1)^2}\right]\Omega. \tag{58}$$

All the off-diagonal matrix elements for transition between different color representations are proportional to Ω:

$$\Sigma_{21} = \langle 6\bar{6}|\hat{\Sigma}|3\bar{3}\rangle = -\frac{N_c^2}{(N_c-1)(N_c^2-1)}\sqrt{\frac{N_c-2}{2(N_c+1)}}\Omega, \tag{59}$$

$$\Sigma_{31} = \langle 15\overline{15}|\hat{\Sigma}|3\bar{3}\rangle = -\frac{N_c^2}{(N_c+1)(N_c^2-1)}\sqrt{\frac{N_c+2}{2(N_c-1)}}\Omega, \tag{60}$$

$$\Sigma_{32} = \langle 15\overline{15}|\hat{\Sigma}|6\bar{6}\rangle = -\frac{1}{2}\cdot\frac{N_c^2}{(N_c^2-1)}\sqrt{\frac{N_c^2-4}{N_c^2-1}}\Omega. \tag{61}$$

Note that the off-diagonal Ω has precisely the same color-dipole structure as the off-diagonal σ_{18} which describes the excitation of the $q\bar{q}$ dipole from the color-singlet to color-octet state [4]. These off-diagonal matrix elements vanish if either $\boldsymbol{r}=0$ or $\boldsymbol{r}'=0$, when the pointlike $|qg\rangle$ and $|q'g'\rangle$ Fock states cannot be resolved.

E. The pointlike triplet, sextet, and 15-plet dipoles and Casimir operators

In the limit of $\boldsymbol{r}=\boldsymbol{r}'=0$, the 4-body states reduce to the pointlike triplet-antitriplet, sextet-antisextet, and 15-$\overline{15}$ dipoles.

Indeed, in this limit

$$\Sigma_{11} = \sigma(\boldsymbol{s}), \tag{62}$$

as expected, while

$$\Sigma_{22} = \frac{3N_c+1}{N_c+1}\sigma(\boldsymbol{s}), \qquad \Sigma_{33} = \frac{3N_c-1}{N_c-1}\sigma(\boldsymbol{s}). \tag{63}$$

The Feynman diagrams of Fig. 5 make it obvious that for partons in the representation R the dipole cross section must be proportional to the Casimir operator C_R. Consequently, the coefficients in (63) must equal the ratio C_R/C_F (a factor C_F for the triplet-antitriplet color dipole had been absorbed into the definition of $\sigma(\boldsymbol{s})$, see Eq. (18)).

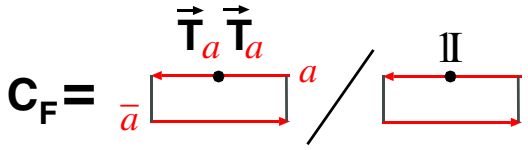

FIG. 10 (color online). The color-flow diagram representation of the quark Casimir operator C_F.

The derivation of C_R by the color-flow diagram technique proceeds as follows:

We recall that the calculation of C_F for the quark a,

$$C_F = \frac{\mathrm{Tr}(\boldsymbol{T}_a \boldsymbol{T}_a)}{\mathrm{Tr}\mathbb{1}}, \tag{64}$$

can be represented in terms of traces of color loop diagrams as shown in Fig. 10. In order to avoid a confusion in the description of the conjugate states, it is convenient to represent the sextet qg state in terms of the three different quark fields,

$$A^i_{kl} = \bar{a}^i(b_k c_l - b_l c_k) + \frac{1}{N_c - 1}[(\bar{a}c)b_l - (\bar{a}b)c_l]\delta^i_k - \frac{1}{N_c - 1}[(\bar{a}c)b_k - (\bar{a}b)c_k]\delta^i_l. \tag{65}$$

One readily finds that

$$\bar{A}A \propto (\bar{a}a)(\bar{b}b)(\bar{c}c) - (\bar{a}a)(\bar{b}c)(\bar{c}b) + \frac{1}{N_c - 1}(\bar{a}c)(\bar{b}a) \times (\bar{c}b) + \frac{1}{N_c - 1}(\bar{a}a)(\bar{b}b)(\bar{c}c) - \frac{1}{N_c - 1}(\bar{a}c) \times (\bar{b}b)(\bar{c}a) - \frac{1}{N_c - 1}(\bar{a}b)(\bar{b}a)(\bar{c}c). \tag{66}$$

In the quark representation the Casimir operator equals

$$(\boldsymbol{T}_b + \boldsymbol{T}_c - \boldsymbol{T}_a)^2 = 3C_F + 2(\boldsymbol{T}_b \boldsymbol{T}_c) - 2(\boldsymbol{T}_a \boldsymbol{T}_b) - 2(\boldsymbol{T}_c \boldsymbol{T}_a). \tag{67}$$

The six color-flow diagrams generated by the expansion (66) are shown in Fig. 11. The straightforward calculation of the corresponding traces, putting the $\boldsymbol{T}_i$ on the relevant horizontal lines in the loops gives

$$C_6 = \frac{3N_c + 1}{N_c + 1} C_F. \tag{68}$$

The similar expansion for the 15-plet state reads

$$\bar{S}S \propto (\bar{a}a)(\bar{b}b)(\bar{c}c) + (\bar{a}a)(\bar{b}c)(\bar{c}b) + \frac{1}{N_c + 1}(\bar{a}c)(\bar{b}a) \times (\bar{c}b) + \frac{1}{N_c + 1}(\bar{a}a)(\bar{b}b)(\bar{c}c) + \frac{1}{N_c + 1}(\bar{a}c) \times (\bar{b}b)(\bar{c}a) + \frac{1}{N_c + 1}(\bar{a}b)(\bar{b}a)(\bar{c}c) \tag{69}$$

and

$$C_{15} = \frac{3N_c - 1}{N_c - 1} C_F. \tag{70}$$

This completes the check of the formulas (63).

F. The $N_c \to -N_c$ transformation between the sextet and 15-plet matrix elements

As a function of N_c, the Casimir operators and matrix elements for transitions containing the sextet and 15-plet states satisfy a curious symmetry

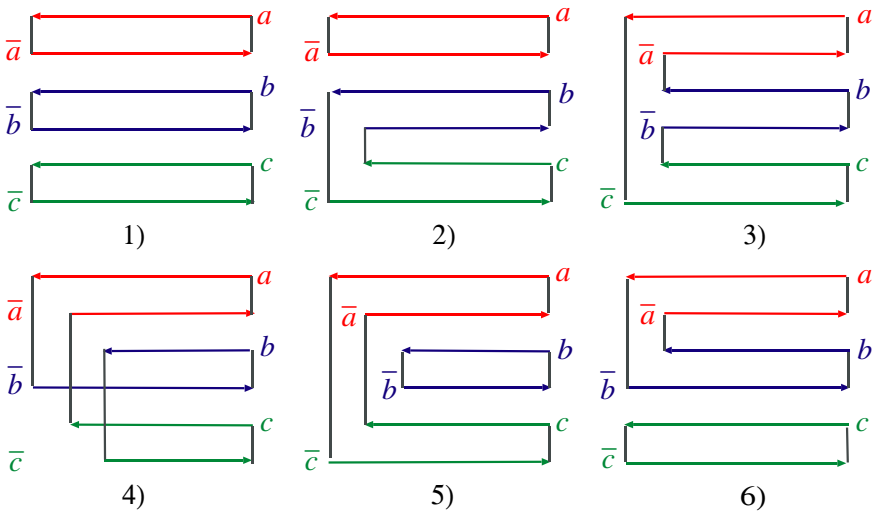

FIG. 11 (color online). The color-flow diagrams for the derivation of the Casimir operator C_F for sextet and 15-plet qg states in the quark-antiquark representation.

$$C_{15}(N_c) = C_6(-N_c), \qquad \Sigma_{33}(N_c) = \Sigma_{22}(-N_c), \qquad \Sigma_{13}(N_c) = -\Sigma_{12}(-N_c). \tag{71}$$

Evidently, the relative minus sign in the last line of (71) is a matter of convention for the basis states. We do not offer any straightforward group-theoretic explanation for this transformation (see, however, a discussion of the correspondence between the symmetric and antisymmetric representations in Cvitanovic's lectures [28]).

G. Large-N_c properties of Σ

The application of the above derived $\hat{\Sigma}$ to the dijet production of the free-nucleon target is straightforward. In the case of the nuclear target one has to solve the secular equation for the eigenvalues and eigenstates of $\hat{\Sigma}$. As a cubic equation, it can be solved in radicals and the corresponding eigenfunctions are directly calculable. The further application of the Sylvester expansion [4] to the S-matrix (31) is then also straightforward. Unfortunately, because of the radicals the relevant Fourier transforms in (13) can only be performed numerically. The direct relationship between the collective nuclear unintegrated gluon density and the dijet spectrum will be lost in such a brute force approach. Furthermore, because the dipole cross section $\sigma(r)$ is a nonanalytic function at $r \to 0$, one faces the menace of a loss of accuracy in numerical evaluations of large Fourier components which are important in the jet cross sections.

Simple algebraic formulas for eigenvalues and analytic results for the dijet spectra which reveal their $k_\perp$-factorization properties are, however, obtained in the large-N_c approximation. Specifically, the diagonalization of the three-channel operator $\hat{\Sigma}$ can readily be accomplished. Furthermore, the resulting Sylvester expansion for the 4-body evolution operator (S-matrix) can be cast into a form which explicitly emphasizes the non-Abelian evolution properties of color dipoles propagating in nuclear matter and furnishes a clear-cut separation of ISI and FSI effects. The higher order terms of expansion in inverse powers of N_c can also be presented in an analytic form [4].

Note that for large N_c

$$\Sigma_{31} = \Sigma_{21} = \frac{1}{N_c\sqrt{2}}\Omega, \qquad \Sigma_{32} = \frac{1}{2}\Omega, \qquad \Sigma_{33} = \Sigma_{22} = 2\sigma(\boldsymbol{s} - \boldsymbol{r}' + \boldsymbol{r}) + \sigma(\boldsymbol{s}) - \frac{1}{2}\Omega, \tag{72}$$

which shows that one must first diagonalize the matrix $\hat{\Sigma}$ in the $|6\bar{6}\rangle$, $|15\overline{15}\rangle$ sector. The two eigenvalues are

$$\Sigma_{2,3} = \sigma_{22} \pm \frac{1}{2}\Omega \tag{73}$$

and the corresponding eigenstates are

$$|2\rangle = \frac{1}{\sqrt{2}}(|6\bar{6}\rangle + |15\overline{15}\rangle) = \frac{V_1}{N_c^{3/2}}, \qquad |3\rangle = \frac{1}{\sqrt{2}}(|6\bar{6}\rangle - |15\overline{15}\rangle) = \frac{V_2}{N_c^{3/2}}. \tag{74}$$

In the basis of the states $|1\rangle = |3\bar{3}\rangle$, $|2\rangle$, and $|3\rangle$ the matrix $\hat{\Sigma}$ takes the form ($\Sigma_1 = \Sigma_{11}$)

$$\hat{\Sigma} = \begin{pmatrix} \Sigma_1 & \frac{1}{N_c}\Omega & 0 \\ \frac{1}{N_c}\Omega & \Sigma_2 & 0 \\ 0 & 0 & \Sigma_3 \end{pmatrix}, \tag{75}$$

where

$$\Sigma_1 = \sigma(\boldsymbol{s} + \boldsymbol{r} - \boldsymbol{r}') + \sigma(\boldsymbol{r}) + \sigma(\boldsymbol{r}'), \qquad \Sigma_2 = 2\sigma(\boldsymbol{s} + \boldsymbol{r} - \boldsymbol{r}') + \sigma(\boldsymbol{s}) = C_2\sigma(\boldsymbol{s} + \boldsymbol{r} - \boldsymbol{r}') + \sigma(\boldsymbol{s}). \tag{76}$$

Here we show an explicit dependence on the Casimir operator for the large-N_c eigenstate

$$C_2 + 1 = \frac{C_6}{C_F} = \frac{C_{15}}{C_F} = 3. \tag{77}$$

As a matter of fact, at large N_c the quark and gluon colors in the sextet and 15-plet states become decorrelated, so that $C_6 = C_{15} = C_A + C_F$ and

$$C_2 = \frac{C_A}{C_F}. \tag{78}$$

To the leading order in the $1/N_c$ expansion, the state $|3\rangle$ is not excited by single-gluon exchange from the initial state $|1\rangle = |3\bar{3}\rangle$, which is obvious also from the projection onto the final states (44), which at large N_c reads

$$\sum_X \langle X| = \sum_R \sqrt{\dim(R)}\langle R\bar{R}| = \sqrt{N_c}\langle 1| + (\sqrt{N_c})^3\langle 2|. \tag{79}$$

In the new basis the non-Abelian intranuclear evolution of the 4-body $qg\bar{q}g'$ state becomes the two-channel problem. Expansion over the final states takes the form

$$\sum_X \langle X|\mathsf{S}[\boldsymbol{b}, \hat{\Sigma}]|1\rangle = \sqrt{N_c}\langle 1|\exp\left[-\frac{1}{2}\hat{\Sigma}T\right]|1\rangle + (\sqrt{N_c})^3 \times \langle 2|\exp\left[-\frac{1}{2}\hat{\Sigma}T\right]|1\rangle. \tag{80}$$

To the leading order in N_c, the S-matrix element in the first term equals

$$\langle 1|\exp\left[-\frac{1}{2}\hat{\Sigma}T\right]|1\rangle = \exp\left[-\frac{1}{2}\Sigma_1 T\right] = \exp\left\{-\frac{1}{2}[\sigma(\boldsymbol{s}) + \sigma(\boldsymbol{r}) + \sigma(\boldsymbol{r}')]T\right\}. \tag{81}$$

Making use of the Sylvester expansion technique used in

[4], for the second matrix element one finds

$$\langle 2|\exp\left[-\frac{1}{2}\hat{\Sigma}T\right]|1\rangle = \Omega\cdot\frac{1}{N_c} \cdot\frac{\exp[-\frac{1}{2}\Sigma_1 T]-\exp[-\frac{1}{2}\Sigma_2 T]}{\Sigma_2-\Sigma_1}. \quad (82)$$

This result is still a too complex one: the dipole-size dependent factor $1/(\Sigma_2-\Sigma_1)$ does not allow any useful Fourier representation of the matrix element (82) in terms of the free-nucleon and collective nuclear gluon densities. This troublesome denominator can be eliminated by the integral representation of Ref. [4],

$$\frac{\exp[-\frac{1}{2}\Sigma_1 T]-\exp[-\frac{1}{2}\Sigma_2 T]}{\Sigma_2-\Sigma_1} = \frac{1}{2}T\int_0^1 d\beta\exp\left[-\frac{1}{2}(\beta\Sigma_1+(1-\beta)\Sigma_2)T\right], \quad (83)$$

where the variable β has a meaning of the depth in nuclear matter from the front face of the nucleus in units of the optical thickness $T(\boldsymbol{b})$. The integral representation (83) makes explicit a decomposition into the ISI and FSI distortions described by the cross sections Σ_1 and Σ_2, respectively. Our final result for the sum over final states reads

$$\sum_X\langle X|\mathsf{S}[\boldsymbol{b},\hat{\Sigma}]|1\rangle = \sum_X\langle X|\exp\left[-\frac{1}{2}\hat{\Sigma}T\right]|1\rangle = \sqrt{N_c}\Big\{\exp\Big[-\frac{1}{2}[\sigma(\boldsymbol{s}+\boldsymbol{r}-\boldsymbol{r}')+\sigma(\boldsymbol{r}) +\sigma(\boldsymbol{r}')]T\Big]+\Omega\cdot T\int_0^1 d\beta \times\exp\left[-\frac{1}{2}(\beta\Sigma_1+(1-\beta)\Sigma_2)T\right]\Big\}. \quad (84)$$

The systematic approach to the $1/N_c$ perturbation expansion has been developed in [4] on an example of quark-antiquark dijets in DIS. Its extension to quark-gluon dijets is straightforward, we will not dwell into that in this communication.

V. THE LINEAR $k_\perp$ FACTORIZATION FOR DIJETS FORM THE FREE-NUCLEON TARGET

The S-matrices in the master formula (13) depend only on the dipole parameters $\boldsymbol{s}$, $\boldsymbol{r}$, $\boldsymbol{r}'$. In the case of the free-nucleon target one can integrate over the overall impact parameter and represent the integrand of Eq. (13) in terms of the dipole cross sections:

$$\begin{aligned}
&2\int d^2\boldsymbol{b}\sum_X\langle X|\{\mathsf{S}^{(4)}_{\bar{q}g'qg}(\boldsymbol{b}'_q,\boldsymbol{b}'_g,\boldsymbol{b}_q,\boldsymbol{b}_g)+\mathsf{S}^{(2)}_{\bar{q}^*q^*}(\boldsymbol{b}',\boldsymbol{b})-\mathsf{S}^{(3)}_{\bar{q}g'q^*}(\boldsymbol{b},\boldsymbol{b}'_q,\boldsymbol{b}'_g)-\mathsf{S}^{(3)}_{\bar{q}^*qg}(\boldsymbol{b}',\boldsymbol{b}_q,\boldsymbol{b}_g)\}|\mathrm{in}\rangle\\
&=\sigma_{\bar{q}^*qg}+\sigma_{q^*\bar{q}g'}-\Sigma_{11}+\sqrt{\frac{\dim(6)}{\dim(3)}}\Sigma_{21}+\sqrt{\frac{\dim(15)}{\dim(3)}}\Sigma_{31}\\
&=\frac{C_A}{C_F}[\sigma(\boldsymbol{s}+\boldsymbol{r}-z\boldsymbol{r}')+\sigma(\boldsymbol{s}+z\boldsymbol{r}-\boldsymbol{r}')-\sigma(\boldsymbol{s}+\boldsymbol{r}-\boldsymbol{r}')-\sigma(\boldsymbol{s}+z\boldsymbol{r}-z\boldsymbol{r}')]-\frac{1}{N_c^2-1}[\sigma(\boldsymbol{s}-z\boldsymbol{r}')+\sigma(\boldsymbol{s}+z\boldsymbol{r})\\
&\quad-\sigma(\boldsymbol{s})-\sigma(\boldsymbol{s}+z\boldsymbol{r}-z\boldsymbol{r}')]+\frac{C_A}{C_F}\Omega. \qquad (85)
\end{aligned}$$

Now we apply the $k_\perp$-factorization representation (19) for the free-nucleon dipole cross section. For instance, one readily finds

$$\Omega=\int d^2\boldsymbol{\kappa}f(\boldsymbol{\kappa})[1-\exp(i\boldsymbol{\kappa}\boldsymbol{r})][1-\exp(-i\boldsymbol{\kappa}\boldsymbol{r}')]\times\exp(i\boldsymbol{\kappa}\boldsymbol{s}). \quad (86)$$

The momentum-space wave function of the qg Fock state of the physical quark is defined by the Fourier transform

$$\Psi(z,\boldsymbol{p})=\int d^2\boldsymbol{r}\Psi(z,\boldsymbol{r})\exp(-i\boldsymbol{p}\boldsymbol{r}). \quad (87)$$

We discuss the cross sections averaged over the helicities of the incident parton and summed over helicities of the final-state partons. Then $\Psi(z,\boldsymbol{p})$ would always enter in combinations of the form [6,16]

$$|\Psi(z,\boldsymbol{p})-\Psi(z,\boldsymbol{p}-\boldsymbol{\kappa})|^2=2N_c\alpha_S(\boldsymbol{p}^2)P_{gq}(z)\cdot\left(\frac{\boldsymbol{p}}{\boldsymbol{p}^2+\varepsilon^2}-\frac{\boldsymbol{p}-\boldsymbol{\kappa}}{(\boldsymbol{p}-\boldsymbol{\kappa})^2+\varepsilon^2}\right)^2, \quad (88)$$

where $P_{gq}(z)$ is the familiar splitting function,

$$P_{gq}(z)=C_F\frac{1+(1-z)^2}{z}, \quad (89)$$

and, neglecting the mass of the incident light quark,

$$\varepsilon^2=z(1-z)(Q^*)^2, \quad (90)$$

where $(Q^*)^2=(\boldsymbol{p}^*)^2$ is the virtuality of the incident quark q^*, given by the square of its transverse momentum $\boldsymbol{p}^*$ in the projectile hadron. If ε^2 is negligible small compared to $\boldsymbol{p}^2$, then one can use the large-$\boldsymbol{p}$ approximation,

$$\left(\frac{\boldsymbol{p}}{\boldsymbol{p}^2}-\frac{\boldsymbol{p}-\boldsymbol{\kappa}}{(\boldsymbol{p}-\boldsymbol{\kappa})^2}\right)^2=\frac{\boldsymbol{\kappa}^2}{\boldsymbol{p}^2(\boldsymbol{p}-\boldsymbol{\kappa})^2}, \quad (91)$$

and it is worth to recall the emerging exact factorization of longitudinal and transverse momentum dependencies which is a well-known feature of the high-energy limit.

Then the master formula for the free-nucleon cross section yields the $k_\perp$-factorization result

$$\frac{d\sigma_N(q^* \to qg)}{dz d^2\boldsymbol{p}_q d^2\boldsymbol{p}_g} = \frac{1}{2(2\pi)^4}\int d^2\boldsymbol{\kappa} f(\boldsymbol{\kappa}) \int d^2\boldsymbol{s} d^2\boldsymbol{r} d^2\boldsymbol{r}' \exp[-i\Delta\boldsymbol{s} - i\boldsymbol{p}\boldsymbol{r} + i\boldsymbol{p}\boldsymbol{r}'] \exp(i\boldsymbol{\kappa}\boldsymbol{s})\Psi(z,\boldsymbol{r})\Psi^*(z,\boldsymbol{r}')$$
$$\times \left\{\frac{C_A}{2C_F}[1-\exp(i\boldsymbol{\kappa}\boldsymbol{r})][1-\exp(-i\boldsymbol{\kappa}\boldsymbol{r}')] + \frac{C_A}{2C_F}[\exp(iz\boldsymbol{\kappa}\boldsymbol{r}) - \exp(i\boldsymbol{\kappa}\boldsymbol{r})][\exp(-iz\boldsymbol{\kappa}\boldsymbol{r}') - \exp(-i\boldsymbol{\kappa}\boldsymbol{r}')]\right.$$
$$\left. - \frac{1}{N_c^2-1}[1-\exp(iz\boldsymbol{\kappa}\boldsymbol{r})][1-\exp(-iz\boldsymbol{\kappa}\boldsymbol{r}')]\right\}$$
$$= \frac{1}{2(2\pi)^2} f(\Delta)\left\{\frac{C_A}{2C_F}|\Psi(z,\boldsymbol{p}) - \Psi(z,\boldsymbol{p}-\Delta)|^2 + \frac{C_A}{2C_F}|\Psi(z,\boldsymbol{p}-\Delta) - \Psi(z,\boldsymbol{p}-z\Delta)|^2\right.$$
$$\left. - \frac{1}{N_c^2-1}|\Psi(z,\boldsymbol{p}) - \Psi(z,\boldsymbol{p}-z\Delta)|^2\right\}. \quad (92)$$

A direct comparison shows that the dijet spectrum (92) on the free nucleon is precisely the differential form of the inclusive single-gluon spectrum from the excitation $q^* \to qg$ which was derived in [6]. The reason emphasized in [18] is that here the excitation $q^* \to qg$ proceeds via one-gluon exchange and the acoplanarity momentum is precisely the transverse momentum of the exchanged gluon. Remarkably, the color-dipole structure of the integrand of the dijet cross section only differs from the one for the single-jet spectrum by the shift of arguments of all the dipole cross sections by $\boldsymbol{s}$.

The free-nucleon cross section is a linear functional of the unintegrated gluon density. Then, with certain reservations on the region of soft Δ, the acoplanarity distribution is a direct probe of $f(x,\Delta)$. First, on the pQCD side, the unintegrated gluon density $f(x,\Delta)$ is well defined only for sufficiently large momenta Δ above the soft scale. Second, from the practical point of view, any definition of the jet momentum has an intrinsic uncertainty with whether the soft hadron belongs to the jet or to the underlying soft event, so that experimentally the acoplanarity momentum is well defined only when it is above the soft scale.

In our previous work on dijets in DIS we noticed that the parton-level dijet spectrum vanishes at $\Delta = 0$, i.e., for exactly back-to-back dijets (see Eq. (45) in Ref. [4]). Precisely the same property holds for the considered quark-gluon jets. Indeed, all the three terms in the curly braces in dijet spectrum (92) vanish identically at $\Delta = 0$, because soft exchanged gluons cannot resolve the quark-gluon Fock state. For the related decoupling of large-wavelength gluons from the color-singlet nucleon, the unintegrated gluon density $f(\Delta)$ is nonsingular at $\Delta = 0$, for instance, see [29] and Eq. (97) below. In the azimuthal correlations the exact dip is observed if the transverse momenta of both jets are of identical magnitude. The dip is accompanied by two symmetric humps at the value of Δ where $\Delta^2 f(\Delta)$ takes the maximal value, the position of the hump depends on the form of $f(\Delta)$. Going from partons to the observed jets will somewhat smear out the dip because of the aforementioned uncertainties in the jet reconstruction. For unequal-momentum jets the dip and the double-hump structure of the dijet spectrum become less pronounced. In the proton-target collision frame, the dip is further filled by the integration over the transverse momentum $\boldsymbol{p}^*$ of the incident valence quark. In the azimuthal correlations of hadron pairs of moderately high transverse momentum experimentally studied at RHIC such a double-hump structure is washed out by the fragmentation of jets.

Now we focus on our major theme: how the linear $k_\perp$ factorization (92) for the dijet production off the free-nucleon target is modified for strongly absorbing nuclear targets.

VI. THE NONLINEAR $k_\perp$ FACTORIZATION FOR THE DIJET PRODUCTION OFF NUCLEI

A. The color-dipole representation at large N_c

The final Fourier representation for the leading term of the large-N_c expansion for the dijet cross section per unit area in the impact-parameter space reads

$$\frac{d\sigma(q^* \to qg)}{d^2\boldsymbol{b} dz d^2\Delta d^2\boldsymbol{p}} = \frac{1}{(2\pi)^4}\int d^2\boldsymbol{s} d^2\boldsymbol{r} d^2\boldsymbol{r}' \times \exp[-i\Delta\boldsymbol{s} - i\boldsymbol{p}\boldsymbol{r} + i\boldsymbol{p}\boldsymbol{r}']\Psi(z,\boldsymbol{r})\Psi^*(z,\boldsymbol{r})\left\{\frac{1}{2}\Omega\cdot T(\boldsymbol{b})\int_0^1 d\beta \exp\left[-\frac{1}{2}[\beta\Sigma_1\right.\right.$$
$$\left.\left. + (1-\beta)\Sigma_2]T(\boldsymbol{b})\right] + \exp\left[-\frac{1}{2}[\sigma(\boldsymbol{s}+\boldsymbol{r}-\boldsymbol{r}') + \sigma(\boldsymbol{r}) + \sigma(\boldsymbol{r}')]T(\boldsymbol{b})\right] + \exp\left[-\frac{1}{2}\sigma(\boldsymbol{s}-z\boldsymbol{r}'+z\boldsymbol{r})T(\boldsymbol{b})\right]$$
$$\left. - \exp\left[-\frac{1}{2}[\sigma(\boldsymbol{r}) + \sigma(\boldsymbol{s}+\boldsymbol{r}-z\boldsymbol{r}')]T(\boldsymbol{b})\right] - \exp\left[-\frac{1}{2}[\sigma(\boldsymbol{r}') + \sigma(\boldsymbol{s}-\boldsymbol{r}'+z\boldsymbol{r})]T(\boldsymbol{b})\right]\right\}. \quad (93)$$

Recall that the first term $\propto \Omega$ describes the excitation from the color-triplet dipole to sextet and 15-plet dipole states. Note how the large-N_c suppression of the off-diagonal matrix element Σ_{12} is compensated for by a large number of final states in the higher representations. At large N_c, once the sextet and 15-plet states have been excited, their deexcitation back to the triplet state is suppressed and the further intranuclear evolution consists of the color rotations within the higher representations. The remaining four terms in (93) describe the rotations within the color-triplet states.

B. Unintegrated collective nuclear glue and isolation of initial-state distortions

The transformation from the color dipole to the momentum representation is furnished by the $k_\perp$-factorization formula (19) and its generalization to the nuclear target. For the latter we adopt the collective nuclear unintegrated gluon density per unit area in the impact-parameter plane, $\phi(\boldsymbol{b}, x, \boldsymbol{\kappa})$, as defined in terms of the nuclear profile function [4,8,30,31]:

$$\Gamma[\boldsymbol{b}, \sigma(x, \boldsymbol{r})] = 1 - \exp\left[-\frac{1}{2}\sigma(x, \boldsymbol{r})T(\boldsymbol{b}) \right] \equiv \int d^2\boldsymbol{\kappa}\phi(\boldsymbol{b}, x, \boldsymbol{\kappa})[1 - \exp(i\boldsymbol{\kappa}\boldsymbol{r})]. \quad (94)$$

The utility of $\phi(\boldsymbol{b}, x, \boldsymbol{\kappa})$ stems from the observation that the driving term of small-x nuclear structure functions, the amplitude of coherent diffractive production of dijets off nuclei, and the single-quark spectrum from the $\gamma^* \to q\bar{q}$ excitation off a nucleus all take the familiar $k_\perp$-factorization form in terms of $\phi(\boldsymbol{b}, x, \boldsymbol{\kappa})$. The so-defined collective nuclear glue $\phi(\boldsymbol{b}, x, \boldsymbol{\kappa})$ satisfies the sum rule

$$\int d^2\boldsymbol{\kappa}\phi(\boldsymbol{b}, x, \boldsymbol{\kappa}) = 1 - \mathsf{S}[\boldsymbol{b}, \sigma_0(x)], \quad (95)$$

where $\sigma_0(x)$ is the dipole cross section for large dipoles. The multiple-scattering expansion of $\phi(\boldsymbol{b}, x, \boldsymbol{\kappa})$ in terms of the collective glue of j-overlapping nucleons in the Lorentz-contracted nucleus and its nuclear shadowing and antishadowing properties are found in [4,8,30,31] and need not be repeated here. We only cite the formula for the so-called saturation scale,

$$Q_A^2(\boldsymbol{b}, x) \approx \frac{4\pi^2}{N_c}\alpha_S(Q_A^2)G(x, Q_A^2)T(\boldsymbol{b}), \quad (96)$$

and reiterate that at a large saturation scale $\phi(\boldsymbol{b}, x, \boldsymbol{\kappa})$ is well defined not only for perturbative values of $\boldsymbol{\kappa}^2$ below $Q_A^2(\boldsymbol{b}, x)$, its continuation to the soft region is also stable,

$$\phi(\boldsymbol{b}, x, \boldsymbol{\kappa}) \approx \frac{1}{\pi}\frac{Q_A^2(\boldsymbol{b}, x)}{(\boldsymbol{\kappa}^2 + Q_A^2(\boldsymbol{b}, x))}. \quad (97)$$

To this end we recall that although $\sigma_0(x)$ enters the multiple-scattering expansion for $\phi(\boldsymbol{b}, x, \boldsymbol{\kappa})$, the final form of $\phi(\boldsymbol{b}, x, \boldsymbol{\kappa})$ is exclusively controlled by $Q_A^2(\boldsymbol{b}, x)$ and does not depend on the auxiliary soft parameter $\sigma_0(x)$ [4]. We also note that the nuclear profile function satisfies the s-channel unitarity bound for the partial waves of the dipole-nucleus scattering, $\Gamma[\boldsymbol{b}, \sigma(x, \boldsymbol{r})] \leq 1$, while the partial wave of the impulse approximation (IA) overshoots the s-channel unitarity bound for a sufficiently heavy nucleus, $\Gamma^{(IA)}[\boldsymbol{b}, \sigma(x, \boldsymbol{r})] = \frac{1}{2}\sigma(x, \boldsymbol{r})T(\boldsymbol{b}) > 1$. As such, the unintegrated collective nuclear gluon density $\phi(\boldsymbol{b}, x, \boldsymbol{\kappa})$ defined by Eq. (94) unitarizes the density of partons in a Lorentz-contracted ultrarelativistic nucleus.

Still another convenient quantity is

$$\Phi(\boldsymbol{b}, x, \boldsymbol{\kappa}) = S[\boldsymbol{b}, \sigma_0(x)]\delta(\boldsymbol{\kappa}) + \phi(\boldsymbol{b}, x, \boldsymbol{\kappa}), \quad (98)$$

in terms of which

$$\exp\left[-\frac{1}{2}\sigma(x, \boldsymbol{r})T(\boldsymbol{b}) \right] = \int d^2\boldsymbol{\kappa}\Phi(\boldsymbol{b}, x, \boldsymbol{\kappa})\exp(i\boldsymbol{\kappa}\boldsymbol{r}). \quad (99)$$

We shall also encounter the collective glue for a slice $[0, \beta]$ of the nucleus:

$$\exp\left[-\frac{1}{2}\beta\sigma(x, \boldsymbol{r})T(\boldsymbol{b}) \right] = \int d^2\boldsymbol{\kappa}\Phi(\beta; \boldsymbol{b}, x, \boldsymbol{\kappa})\exp(i\boldsymbol{\kappa}\boldsymbol{r}), \quad (100)$$

and the intranuclear attenuation-distorted wave function in the dipole and momentum representations,

$$\Psi(\beta, x; z, \boldsymbol{r}) = \Psi(z, \boldsymbol{r})\exp\left[-\frac{1}{2}\beta\sigma(x, \boldsymbol{r})T(\boldsymbol{b}) \right],$$
$$\Psi(\beta, x; z, \boldsymbol{p}) = \int d^2\boldsymbol{r}\Psi(\beta; z, \boldsymbol{r})\exp(-i\boldsymbol{p}\boldsymbol{r}) = \int d^2\boldsymbol{\kappa}\Psi(z, \boldsymbol{p} - \boldsymbol{\kappa})\Phi(\beta; \boldsymbol{b}, x, \boldsymbol{\kappa}). \quad (101)$$

Hereafter, unless it may cause confusion, we suppress the variable x in gluon densities, dipole cross sections, and distorted wave functions.

C. Excitation of color-triplet quark-gluon dipoles

First, we rewrite the last four terms in the integrand of (93) in terms of the distorted wave functions. Then we make use of the Fourier representation (99), (101):

$$\left.\frac{d\sigma(q^*\to qg)}{d^2\boldsymbol{b}dzd^2d^2\boldsymbol{p}}\right|_3 = \frac{1}{(2\pi)^4}\int d^2\boldsymbol{s}d^2\boldsymbol{r}d^2\boldsymbol{r}'\exp[-i\Delta\boldsymbol{s}-i\boldsymbol{p}\boldsymbol{r}+i\boldsymbol{p}\boldsymbol{r}']\Big\{\Psi(1;z,\boldsymbol{r})\Psi^*(1;z,\boldsymbol{r}')\exp\Big[-\frac{1}{2}\sigma(\boldsymbol{s}+\boldsymbol{r}-\boldsymbol{r})T(\boldsymbol{b})\Big]$$
$$+\Psi(z,\boldsymbol{r})\Psi^*(z,\boldsymbol{r}')\exp\Big[-\frac{1}{2}\sigma(\boldsymbol{s}-z\boldsymbol{r}'+z\boldsymbol{r})T(\boldsymbol{b})\Big]-\Psi(1;z,\boldsymbol{r})\Psi^*(z,\boldsymbol{r}')\exp\Big[-\frac{1}{2}\sigma(\boldsymbol{s}+\boldsymbol{r}-z\boldsymbol{r}')T(\boldsymbol{b})\Big]$$
$$-\Psi(z,\boldsymbol{r})\Psi^*(1;z,\boldsymbol{r}')\exp\Big[-\frac{1}{2}\sigma(\boldsymbol{s}-\boldsymbol{r}'+z\boldsymbol{r})T(\boldsymbol{b})\Big]\Big\}$$
$$=\frac{1}{(2\pi)^4}\int d^2\boldsymbol{s}d^2\boldsymbol{r}d^2\boldsymbol{r}'d^2\boldsymbol{\kappa}\Phi(\boldsymbol{b},\boldsymbol{\kappa})\exp[-i\Delta\boldsymbol{s}-i\boldsymbol{p}\boldsymbol{r}+i\boldsymbol{p}\boldsymbol{r}']\Big\{\Psi(1;z,\boldsymbol{r})\Psi^*(1;z,\boldsymbol{r}')\exp[i\boldsymbol{\kappa}(\boldsymbol{s}+\boldsymbol{r}-\boldsymbol{r}')]$$
$$+\Psi(z,\boldsymbol{r})\Psi^*(z,\boldsymbol{r}')\exp[i\boldsymbol{\kappa}(\boldsymbol{s}-z\boldsymbol{r}'+z\boldsymbol{r})]-\Psi(1;z,\boldsymbol{r})\Psi^*(z,\boldsymbol{r}')\exp[i\boldsymbol{\kappa}(\boldsymbol{s}+\boldsymbol{r}-z\boldsymbol{r}')]$$
$$-\Psi(z,\boldsymbol{r})\Psi^*(1;z,\boldsymbol{r}')\exp[i\boldsymbol{\kappa}(\boldsymbol{s}-\boldsymbol{r}'+z\boldsymbol{r})]\Big\}$$
$$=\frac{1}{(2\pi)^2}\Phi(\boldsymbol{b},\Delta)|\Psi(1;z,\boldsymbol{p}-\Delta)-\Psi(z,\boldsymbol{p}-z\Delta)|^2$$
$$=\frac{1}{(2\pi)^2}\phi(\boldsymbol{b},\Delta)|\Psi(1;z,\boldsymbol{p}-\Delta)-\Psi(z,\boldsymbol{p}-z\Delta)|^2+\frac{1}{(2\pi)^2}\delta(\Delta)|\Psi(1;z,\boldsymbol{p})-\Psi(z,\boldsymbol{p})|^2\mathsf{S}[\boldsymbol{b},\sigma_0(x)]. \quad (102)$$

Now recall [8] that the amplitude of the coherent diffractive excitation $qA\to(qg)A$ is precisely proportional to

$$\Psi(z,\boldsymbol{p})-\Psi(1;z,\boldsymbol{p}) = \int d^2\boldsymbol{r}\Psi(z,\boldsymbol{r})\Big\{1-\exp\Big[-\frac{1}{2}\sigma(\boldsymbol{r})T(\boldsymbol{b})\Big]\Big\}\exp[-i\boldsymbol{p}\boldsymbol{r}], \quad (103)$$

so that the last term in (102) describes the coherent diffractive production of dijets. In the approximation of a very large nucleus the diffractive dijets are produced exactly back-to-back. For finite nuclei instead of the delta-function $\delta(\Delta)$ one finds a sharp peak of the width $\Delta^2\lesssim 1/R_A^2$ which is described by the form factor of the nucleus, the details are found in [8] and must not be repeated here. The first term in (102) describes inelastic, incoherent production of color-triplet qg states.

D. The contribution from sextet and 15-plet final states

The evaluation of the contribution from the excitation of higher color representations in (93) proceeds as follows. First, we make use of the integral representation (86) for the off-diagonal cross section. Second, keeping an explicit dependence on the Casimir operators $C_{6,15}$ (cf. Eq. (77)), we have

$$\int_0^1 d\beta\exp\Big[-\frac{1}{2}(\beta\Sigma_1+(1-\beta)\Sigma_2)T(\boldsymbol{b})\Big] = \int_0^1 d\beta\exp\Big\{-\frac{1}{2}\beta[\sigma(\boldsymbol{s}+\boldsymbol{r}-\boldsymbol{r}')+\sigma(\boldsymbol{r})+\sigma(\boldsymbol{r}')]T(\boldsymbol{b})\Big\}$$
$$\times\exp\Big\{-\frac{1}{2}(1-\beta)[C_2\sigma(\boldsymbol{s}+\boldsymbol{r}-\boldsymbol{r}')+\sigma(\boldsymbol{s})]T(\boldsymbol{b})\Big\}$$
$$=\int_0^1 d\beta\exp\Big[-\frac{1}{2}\beta\sigma(\boldsymbol{r})T(\boldsymbol{b})\Big]\exp\Big[-\frac{1}{2}\beta\sigma(\boldsymbol{r}')T(\boldsymbol{b})\Big]$$
$$\times\int d^2\boldsymbol{\kappa}_3\Phi(\beta;\boldsymbol{b},\boldsymbol{\kappa}_3)\exp[i\boldsymbol{\kappa}_3(\boldsymbol{s}+\boldsymbol{r}-\boldsymbol{r}')]$$
$$\times\int d^2\boldsymbol{\kappa}_2\Phi(C_2(1-\beta);\boldsymbol{b},\boldsymbol{\kappa}_2)\exp[i\boldsymbol{\kappa}_2(\boldsymbol{s}+\boldsymbol{r}-\boldsymbol{r}')]$$
$$\times\int d^2\boldsymbol{\kappa}_1\Phi(1-\beta;\boldsymbol{b},\boldsymbol{\kappa}_1)\exp[i\boldsymbol{\kappa}_1\boldsymbol{s}]. \quad (104)$$

In this decomposition we keep the dipole form of the two attenuation factors $\mathsf{S}[\boldsymbol{b},\beta\sigma(\boldsymbol{r})]$ and $\mathsf{S}[\boldsymbol{b},\beta\sigma(\boldsymbol{r}')]$. They describe the coherent distortion of the color-triplet quark-gluon dipole by intranuclear ISI before the excitation into the sextet and 15-plet representations at the depth β from the front face of the nucleus. The way to handle these distortion factors has already been clarified above. Note that in contrast to the quark-antiquark dijet production in DIS off nuclei, both the ISI and FSI distortion factors depend on the dipole parameter $\boldsymbol{s}$ and explicitly contribute to the acoplanarity distribution.

Combining together (86), (101), and (104) we obtain the dijet spectrum from the excitation of the sextet and 15-plet dipoles

$$\left.\frac{d\sigma(q^*\to qg)}{d^2\boldsymbol{b}dzd^2\Delta d^2\boldsymbol{p}}\right|_{6+15}=\frac{1}{(2\pi)^2}T(\boldsymbol{b})\int_0^1 d\beta\times\int d^2\boldsymbol{\kappa}d^2\boldsymbol{\kappa}_1d^2\boldsymbol{\kappa}_2d^2\boldsymbol{\kappa}_3\delta(\boldsymbol{\kappa}+\boldsymbol{\kappa}_1+\boldsymbol{\kappa}_2+\boldsymbol{\kappa}_3-\Delta)$$
$$\times f(\boldsymbol{\kappa})\Phi(1-\beta;\boldsymbol{b},\boldsymbol{\kappa}_1)\Phi(C_2(1-\beta);\boldsymbol{b},\boldsymbol{\kappa}_2)\Phi(\beta;\boldsymbol{b},\boldsymbol{\kappa}_3)$$
$$\times|\Psi(\beta;z,\boldsymbol{p}-\boldsymbol{\kappa}_1)-\Psi(\beta;z,\boldsymbol{p}-\boldsymbol{\kappa}_1-\boldsymbol{\kappa}_2)|^2. \quad (105)$$

The acoplanarity momentum Δ manifestly receives four distinct contributions which can be classified as follows. The excitation from the color triplet to the sextet and 15-plet states by single-gluon exchange with one of the nucleons of the nucleus contributes the transverse momentum $\boldsymbol{\kappa}$. The momentum $\boldsymbol{\kappa}_3$ comes from the ISI of the incident quark, the FSI of the qg dipole in the sextet, and 15-plet representations contributes $\boldsymbol{\kappa}_1$ and $\boldsymbol{\kappa}_2$.

There are several crucial points about the explicit result (105). First, it is a quadrature in terms of the collective nuclear glue. Such a nonlinear $k_\perp$-factorization representation would have been impossible without the transformation of Ref. [4] from the Sylvester expansion (82) to the integral representation (83). Second, it contains the free-nucleon unintegrated glue and the collective nuclear glue defined for the slices of the nucleus $[0,\beta]$ in which the ISI takes place and $[\beta,1]$ in which the FSI takes place rather than the collective glue defined for whole nucleus, i.e, the slice $[0,1]$. Third, the emergence of the collective nuclear glue $\Phi(C_2(1-\beta);\boldsymbol{b},\boldsymbol{\kappa}_2)$ is not accidental: $(1-\beta)$ is a thickness of the slice $[\beta,1]$ of the nuclear matter traversed by the sextet and 15-plet qg dipoles, while the factor C_2 derives from the Casimir operators of higher representations, see Eq. (77). That is one more illustration of our point [4,6] that the collective gluon field of the nucleus cannot be described by a single function, rather it is a density matrix in the space of color representations. In the considered large-N_c approximation, $C_2=C_A/C_F$ and $\Phi((1-\beta)C_A/C_F;\boldsymbol{b},\boldsymbol{\kappa}_2)$ is precisely the collective nuclear glue defined in terms of the color-singlet gluon-gluon dipole.

Fourth, although the exponentials in the numerator of the Sylvester expansion (82) could have been cast as Fourier representations in terms of the collective glue for the whole nucleus, that would not yield any useful quadratures for the dijet spectrum the straightforward Fourier representation of the factor $1/(\Sigma_2-\Sigma_1)$ in terms of the unintegrated gluon densities is impossible. The brute force calculation of Fourier transforms from the dipole to the momentum space is possible but would miss all the crucial features of the nonlinear $k_\perp$ factorization (105): the clear-cut link to the non-Abelian intranuclear evolution of color dipoles in a nucleus, its decomposition into the ISI and FSI effects in terms of the collective glue for slices of the nucleus, the interplay of coherent and incoherent ISI's, the explicit dependence of FSI on the Casimir operators for different partons from the relevant pQCD subprocess.

The ISI and FSI distortions can partly be combined taking the convolution [4]

$$\int d^2\boldsymbol{\kappa}_3d^2\boldsymbol{\kappa}_2\Phi(C_2(1-\beta);\boldsymbol{b},\boldsymbol{\kappa}_2)\Phi(\beta;\boldsymbol{b},\boldsymbol{\kappa}_3)\delta(\boldsymbol{\kappa}-\boldsymbol{\kappa}_2-\boldsymbol{\kappa}_3)$$
$$=\Phi(\beta+C_2(1-\beta);\boldsymbol{b},\boldsymbol{\kappa}), \quad (106)$$

which is also obvious from the color-dipole form in (104).

E. Nonlinear $k_\perp$ factorization for dijets: the universality classes

1. Quark-gluon vs quark-antiquark dijets

After application of the convolution (106), the final result for the inclusive quark-gluon dijet spectrum takes the form

$$\frac{(2\pi)^2d\sigma_A(q^*\to qg)}{d^2\boldsymbol{b}dzd^2\boldsymbol{p}d^2\Delta}=\frac{1}{2}T(\boldsymbol{b})\int_0^1 d\beta\int d^2\boldsymbol{\kappa}_1d^2\boldsymbol{\kappa}f(x,\boldsymbol{\kappa})\times\Phi(1-\beta,\boldsymbol{b},x,\Delta-\boldsymbol{\kappa}_1-\boldsymbol{\kappa})\Phi(\beta+C_2(1-\beta),\boldsymbol{b},x,\boldsymbol{\kappa}_1)$$
$$\times|\Psi(\beta;z,\boldsymbol{p}-\boldsymbol{\kappa}_1)-\Psi(\beta;z,\boldsymbol{p}-\boldsymbol{\kappa}_1-\boldsymbol{\kappa})|^2+\phi(\boldsymbol{b},x,\Delta)|\Psi(1;z,\boldsymbol{p}-\Delta)-\Psi(z,\boldsymbol{p}-z\Delta)|^2$$
$$+\delta(\Delta)\mathsf{S}[\boldsymbol{b},\sigma_0(x)]|\Psi(1;z,\boldsymbol{p})-\Psi(z,\boldsymbol{p})|^2, \quad (107)$$

which must be compared to the large-N_c version of the free-nucleon cross section (92). The free-nucleon cross section satisfies the linear $k_\perp$ factorization—it is a linear functional of the unintegrated gluon density. The $k_\perp$-factorization properties of the nuclear cross section are much more complicated.

At this point, it is instructive to discuss (107) in conjunction with the quark-antiquark dijet spectrum in DIS [4] and gluon-nucleus collisions [18]. The spectrum of dijets in DIS equals

$$\frac{(2\pi)^2d\sigma_A(\gamma^*\to Q\bar{Q})}{d^2\boldsymbol{b}dzd^2\boldsymbol{p}d^2\Delta}=\frac{1}{2}T(\boldsymbol{b})\int_0^1 d\beta\int d^2\boldsymbol{\kappa}_1d^2\boldsymbol{\kappa}\times f(\boldsymbol{\kappa})\Phi(1-\beta,\boldsymbol{b},\Delta-\boldsymbol{\kappa}_1-\boldsymbol{\kappa})\Phi(1-\beta,\boldsymbol{b},\boldsymbol{\kappa}_1)$$
$$\times|\Psi(\beta;z,\boldsymbol{p}-\boldsymbol{\kappa}_1)-\Psi(\beta;z,\boldsymbol{p}-\boldsymbol{\kappa}_1-\boldsymbol{\kappa})|^2+\delta(\Delta)|\Psi(1;z,\boldsymbol{p})-\Psi(z,\boldsymbol{p})|^2, \quad (108)$$

where the first term describes the excitation of the color dipole from the lower (color-singlet) to higher (octet)

representation, whereas the second term is the contribution from coherent diffractive excitation. Here $\Psi(z, \boldsymbol{p})$ stands for the wave function of the $q\bar{q}$ Fock state of the photon [6,16].

Still another reference observable is the spectrum of the quark-antiquark dijets in gA collisions,

$$\frac{(2\pi)^2 d\sigma_A(g^* \to Q\bar{Q})}{dz d^2\boldsymbol{p} d^2\boldsymbol{b} d^2\Delta} = \int d^2\boldsymbol{\kappa}\Phi(1;\boldsymbol{b},\boldsymbol{\kappa})\Phi(1;\boldsymbol{b},\Delta-\boldsymbol{\kappa}) \times |\Psi(z,\boldsymbol{p}-\boldsymbol{\kappa}) - \Psi(z,\boldsymbol{p}-z\Delta)|^2, \quad (109)$$

where $\Psi(z, \boldsymbol{p})$ stands for the wave function of the $q\bar{q}$ Fock state of the gluon [6,16].

Now we can identify the four universality classes of the nonlinear $k_\perp$ factorization which differ by the pattern of transitions between the initial and final-state color multiplets. They describe the leading transitions in the large-N_c approximation, the excitation and regeneration processes to higher orders in $1/N_c$ satisfy the nonlinear $k_\perp$ factorization of still higher nonlinearity in gluon densities, the examples are found in [4].

2. Excitation of higher color representations from partons in the lower representations

Excitation of color-octet states in DIS, and of sextet and 15-plet states in qA interactions, belong to this universality class. The two reactions have much similarity. In both cases, the $\propto 1/N_c$ suppression of the transition matrix element is compensated for the number of states in higher representations which is by the factor N_c^2 larger than in the lower representation. In both cases the hard transition from the lower to higher color representations is described by the free-nucleon gluon density $f(x, \boldsymbol{\kappa})$ rather than the collective nuclear glue. In $q\bar{q}$ excitation in DIS the corresponding contribution to the dijet spectrum is the fifth order functional of gluon densities. In the qg case it is the sixth order functional of gluon densities, only after the application of the convolution (106) it takes the form of the fifth order functional. In both cases two powers of the collective nuclear glue enter implicitly via the coherent ISI distortions of the wave function $\Psi(\beta; z, \boldsymbol{p})$ in the slice of the nuclear matter $[0, \beta]$ before the excitation of color dipoles in the higher representation, two more powers of the collective nuclear glue describe the broadening of the acoplanarity distribution by incoherent ISI and FSI.

The principal difference between DIS and qA interactions is in the nuclear thickness dependence of the incoherent distortion factors. Namely, the factor

$$\Phi((1-\beta),\boldsymbol{b},\Delta-\boldsymbol{\kappa}_1-\boldsymbol{\kappa})\Phi((1-\beta),\boldsymbol{b},\boldsymbol{\kappa}_1)$$

in DIS is a symmetric function of the nuclear gluon momenta $\boldsymbol{\kappa}_1$ and $\boldsymbol{\kappa}_2 = \Delta - \boldsymbol{\kappa}_1 - \boldsymbol{\kappa}$ which flow from the nucleus to the quark and antiquark (or vice versa), respectively. It describes equal and uncorrelated distortion of the outgoing quark and antiquark waves by pure FSI. Such an uncorrelated incoherent final-state distortion is a feature of the large N_c approximation. For qg dijets in qA collisions the distortion factor

$$\Phi(1-\beta,\boldsymbol{b},\boldsymbol{\kappa}_2)\Phi(C_2(1-\beta)+\beta,\boldsymbol{b},\boldsymbol{\kappa}_1)$$

after the convolution (106) is an asymmetric one. The first source of the asymmetry is the nonsinglet color charge of the projectile parton. The second source is that the two partons in the final state belong to different color representations. This is best seen from in the overall distortion factor in (105),

$$\Phi(\beta;\boldsymbol{b},\boldsymbol{\kappa}_3)\Phi(C_2(1-\beta);\boldsymbol{b},\boldsymbol{\kappa}_2)\Phi(1-\beta;\boldsymbol{b},\boldsymbol{\kappa}_1),$$

before taking the convolution (106). The FSI distortions in the slice $(1-\beta)$ of the nucleus are given by the two last factors, of which $\Phi(1-\beta;\boldsymbol{b},\boldsymbol{\kappa}_1)$ is a broadening due to final-state rescatterings of the quark. Because $C_2 = C_A/C_F$, see Eq. (78), the second FSI factor, $\Phi(C_2(1-\beta);\boldsymbol{b},\boldsymbol{\kappa}_2)$, corresponds to the FSI distortion of exactly the outgoing gluon wave. To the large-N_c approximation the rescatterings of the quark and gluon are uncorrelated.

The coherent ISI distortion of the wave functions in DIS and qA collisions is identical. However, in qA collisions this coherent distortion is accompanied by an incoherent ISI distortion of the incident quark wave described by $\Phi(\beta;\boldsymbol{b},\boldsymbol{\kappa}_3)$. In DIS the incoherent ISI distortions are absent because the photon is a color-singlet particle. We can anticipate that gluon-nucleus collisions with excitation of gluon-gluon dijets in higher color representations will belong to this universality class.

3. Excitation of final-state dipoles in exactly the same color state as the incident parton: coherent diffraction

To this universality class belong the exactly back-to-back dijets. The experimental signature of the coherent diffraction is a retention of the target nucleus in the ground state and large rapidity gap between the hadronic debris of the diffractive dijet and the recoil nucleus. It is most important for DIS where coherent diffraction dissociation of the photon into $q\bar{q}$ dijets makes for heavy nuclei $\approx 50\%$ of the total DIS rate [32]. The origin of the coherent diffraction is a coherent nuclear distortion of the wave function of the $q\bar{q}$ Fock state over the whole thickness of the nucleus.

In the coherent diffractive excitation of qg dipoles in qA collisions the qg dipole must propagate in exactly the same color state as the incident quark. The nuclear suppression factor $\mathsf{S}[\boldsymbol{b}, \sigma_0(x)]$ has the meaning of

$$\mathsf{S}[\boldsymbol{b},\sigma_0(x)] = \left(\mathsf{S}\left[\boldsymbol{b},\frac{1}{2}\sigma_0(x)\right]\right)^2 \quad (110)$$

and the factor $\mathsf{S}[\boldsymbol{b}, \frac{1}{2}\sigma_0(x)]$ in the diffractive amplitude corresponds to the intranuclear attenuation of the quark wave with the total cross section

$$\sigma_{qN} = \frac{1}{2}\sigma_0(x). \tag{111}$$

Coherent diffractive excitation of color-octet gluon-gluon dijets in gluon-nucleus collisions is expected to exhibit similar properties.

Coherent diffractive excitation of $Q\bar{Q}$ dipoles in gA collisions is allowed, but it is suppressed at large N_c by the condition that the $Q\bar{Q}$ dipole must propagate in exactly the same color state as the incident gluon.

4. Incoherent excitation of final-state dipoles in the same lower color representation as the incident parton

An example of this universality class is an inelastic excitation of color-triplet qg states in qA collisions followed by a color excitation of the target. Here both the incident parton and dijet belong to the fundamental, i.e., lower, representation of $SU(N_c)$. The intranuclear evolution of such a dipole is confined to rotations within the color-triplet state. This contribution is not suppressed at large N_c. The dijet cross section for this universality class looks like satisfying the linear $k_\perp$ factorization in terms of $\phi(\boldsymbol{b}, x, \boldsymbol{\kappa})$. But this is not the case: one of the wave functions, $\Psi(1; z, \boldsymbol{p}_g)$, is coherently distorted over the whole thickness of the nucleus, so that this contribution is a cubic functional of the collective nuclear glue. The striking feature of this universality class is a complete absence of the incoherent initial and final-state interaction effects.

We can anticipate that gluon-nucleus collisions with excitation of color-octet gluon-gluon dijets will belong to this universality class, although one has to account for the existence of the two, F-coupled and D-coupled, octet states.

Although superficially it looks like a subclass of this universality class, the coherent diffraction is a distinct class for the property of the exact back-to-back dijets and the rapidity gap between the dijet and the recoil nucleus in the ground state.

5. Excitation of final-state dipoles in the same higher color representation as the incident parton

In the realm of QCD with gluons in the adjoint representation and quarks in the fundamental representation, this universality class is exhausted by the quark-antiquark dijets in gluon-nucleus collisions. Only in this case the initial parton (gluon) belongs to the higher (octet) color multiplet of the final $Q\bar{Q}$ state. At large N_c, the intranuclear evolution of $Q\bar{Q}$ will consist of color rotations within the space of color-octet states. The deexcitation from the color-octet to color-singlet $Q\bar{Q}$ dipoles is suppressed at large N_c. Consequently, the non-Abelian evolution of the $Q\bar{Q}Q'\bar{Q}'$ state becomes the single-channel problem. The coherent diffraction excitation, in which the initial and final color states must be identical, is likewise suppressed. The emerging pattern of quadratic nonlinearity can be related to the large-N_c gluon behaving like the color-uncorrelated quark and antiquark. A remarkable absence of coherent distortions of the wave function of the $c\bar{c}$ Fock state is noteworthy.

The above classification exhausts reactions caused by incident photons, quarks, and gluons. However, technically all the universality classes have a much broader basis. Indeed, instead of an incident gluon one can think of the projectile which is a compact lump of many partons in the highest possible color representation. For instance, compact sextet diquarks are possible.

6. Is an experimental separation of events belonging to different universality classes possible?

First we note that in none of the universality classes the dijet cross section factorizes into the hard excitation of the dijet in the collective nuclear glue accompanied by the incoherent initial and final-state interactions of partons. Coherent diffraction has distinct signatures and the experimental separation of events from this universality class is not a problem. Production of very forward dijets in proton-nucleus collisions evidently tags quark-nucleus collisions. Production of open charm in the proton hemisphere of the proton-nucleus collisions tags gluon-nucleus collisions. Incoherent processes belonging to different universality classes are characterized by distinct color charge of the hard dijet and this distinction is well defined at the parton level. Translating the cross talk between color charges in the dijet, the spectator partons of the proton, and the color-excited nucleus remnant into properties of hadronic final states can only be done within nonperturbative hadronization models, though. As an example we cite the impact of color reconnection effects on the flow of slow hadrons and the accuracy of the $W^\pm$ mass determination in e^+e^- annihilation ([33], for the review see [34]).

F. The impulse approximation

In the impulse approximation (IA) one only has to keep the terms linear in $T(\boldsymbol{b})$. The transition to the IA is best seen in the color-dipole representation (93). Recall, that our formulas for nuclear cross section were derived in the large-N_c approximation. Here the first term, the contribution from the sextet and 15-plet final states, is already linear in $T(\boldsymbol{b})$ and one must put the attenuation factors equal to unity. The remaining four exponentials must be expanded to terms linear in $T(\boldsymbol{b})$. Then one would find precisely the large-N_c version of Eq. (85) times $T(\boldsymbol{b})$. The integration over impact parameters gives $\int d^2\boldsymbol{b}T(\boldsymbol{b}) = A$. Such a comparison does not expose the role of coherent diffraction and we revisit the issue in the momentum representation.

We start with the sextet and 15-plet contribution in (107). It already contains the factor $T(\boldsymbol{b})$. Consequently, one must neglect ISI distortions in the wave function $\Psi(\beta; z, \boldsymbol{p}) \Rightarrow \Psi(z, \boldsymbol{p})$ and take

$$\Phi(1-\beta, \boldsymbol{b}, x, \Delta-\boldsymbol{\kappa}_1-\boldsymbol{\kappa})\Phi(2-\beta, \boldsymbol{b}, x, \boldsymbol{\kappa}_1) = \delta(\Delta-\boldsymbol{\kappa}_1-\boldsymbol{\kappa})\delta(\boldsymbol{\kappa}_1). \quad (112)$$

This way one would recover the first term in the right-hand side (rhs) of Eq. (92). In the contribution from the excitation of the triplet dipoles one must neglect the distortion of the wave function and take

$$\phi(\boldsymbol{b}, x, \boldsymbol{\kappa}) = \frac{1}{2}T(\boldsymbol{b})f(x, \boldsymbol{\kappa}). \quad (113)$$

The second term in the rhs of Eq. (92) is recovered. Finally, according to Eq. (103) the diffractive amplitude starts with the term linear in $T(\boldsymbol{b})$. Consequently, the coherent diffractive contribution to the dijet cross spectrum starts with the terms $\propto T^2(\boldsymbol{b})$ and vanishes in the IA.

VII. NUCLEAR BROADENING OF THE ACOPLANARITY DISTRIBUTION AND THE BACK-TO-BACK DIP

The nuclear broadening of the acoplanarity distribution of hard quark-gluon dijets from qA collisions is somewhat different from the broadening of quark-antiquark jets in DIS and now we comment on those differences.

A. Coherent diffractive contribution

The first striking difference is in the role of the coherent diffractive production. It gives exactly back-to-back dijets. In the considered approximation of single-gluon exchange in the t-channel diffractive production off the free-nucleon target vanishes. Experimentally, at Hadron Electron Ring Accelerator (HERA) energies a fraction of DIS which is diffractive does not exceed 10% [35]. In contrast to that, in DIS off heavy nuclei a fraction of coherent diffraction was shown to be as large as $\approx 50\%$ [32]. The existence of coherent diffractive mechanism in the quark-nucleus collisions is interesting by itself. From the practical point of view, it is suppressed by nuclear absorption and is marginal.

B. Excitation of the color-triplet states

Inelastic excitation of color-triplet dipoles is a specific feature of qA collisions in the sense that it has no counterpart in DIS. One must compare

$$\phi(\boldsymbol{b}, x, \Delta)|\Psi(1; z, \boldsymbol{p}-\Delta) - \Psi(z, \boldsymbol{p}-z\Delta)|^2 \quad (114)$$

with its IA form

$$\frac{1}{2}T(\boldsymbol{b})f(\Delta)|\Psi(z, \boldsymbol{p}-\Delta) - \Psi(z, \boldsymbol{p}-z\Delta)|^2. \quad (115)$$

The first striking distinction is that for the free-nucleon target the contribution of this process vanishes at $z \to 1$, when the incident quark's momentum is transferred entirely to the forward gluon jet. For the nuclear target this is not the case because one of the wave functions in (114) is the nuclear-distorted one. Because $\boldsymbol{p}-\Delta = -\boldsymbol{p}_q$, it takes the form $\phi(\boldsymbol{b}, x, \Delta)|\Psi(1; z, \boldsymbol{p}_q) - \Psi(z, \boldsymbol{p}_q)|^2$; as a function of the quark-jet momentum, it is reminiscent of the coherent diffractive contribution, but the acoplanarity momentum distribution is given by the unintegrated nuclear gluon density $\phi(\boldsymbol{b}, x, \Delta)$. Hereafter we consider the case of finite $(1-z)$.

A comprehensive discussion of nuclear properties of the ratio

$$R_g(\boldsymbol{b}, \Delta) = \frac{2\phi(\boldsymbol{b}, x, \Delta)}{T(\boldsymbol{b})f(\Delta)} \quad (116)$$

is found in [4,6]. It is nuclear-shadowed, $R_g(\boldsymbol{b}, \Delta) < 1$, for $\Delta^2 \lesssim Q_A^2(\boldsymbol{b})$ and it exhibits antishadowing property $R_g(\boldsymbol{b}, \Delta) > 1$ in a broad region of $\Delta^2 \gtrsim Q_A^2(\boldsymbol{b})$. The maximum value of $R_g(\boldsymbol{b}, \Delta)$ is reached at a value of Δ^2 which is larger than $Q_A^2(\boldsymbol{b})$ by a large numerical factor.

Now we turn to distortions of the wave function. We are interested in hard dijets. If the incident quark is a valence quark of the proton, its transverse momentum and virtuality have the hadronic scale and can be neglected. For hard jets

$$\Psi(z, \boldsymbol{p}) \propto \frac{\boldsymbol{p}}{\boldsymbol{p}^2} \quad (117)$$

and, upon averaging over the azimuthal angle φ of the gluon momentum $\boldsymbol{\kappa}$,

$$\langle\Psi(z, \boldsymbol{p}-\boldsymbol{\kappa})\rangle_\varphi \propto \frac{\boldsymbol{p}}{\boldsymbol{p}^2}\theta(\boldsymbol{p}^2-\boldsymbol{\kappa}^2). \quad (118)$$

Consequently, the wave function distortion factor equals

$$\rho_\psi(\boldsymbol{b}, z, \boldsymbol{p}) = \frac{\Psi(1; z, \boldsymbol{p})}{\Psi(z, \boldsymbol{p})} = \int^{\boldsymbol{p}^2} d^2\boldsymbol{\kappa}\Phi(\boldsymbol{b}, x, \boldsymbol{\kappa}) = 1 - \int_{\boldsymbol{p}^2} d^2\boldsymbol{\kappa}\Phi(\boldsymbol{b}, x, \boldsymbol{\kappa}). \quad (119)$$

For the weakly virtual incident quark it does not depend on z. For hard jets, $\boldsymbol{p}^2 \gtrsim Q_a^2(\boldsymbol{b})$, the remaining integral (119) can be evaluated following the analysis of the Cronin effect in [6]. Namely, here we can use the leading-twist approximation,

$$\Phi(\boldsymbol{b}, x, \boldsymbol{\kappa}) = \frac{1}{2}T(\boldsymbol{b})f(\boldsymbol{\kappa}), \quad (120)$$

and the definition (20) with the result

$$\delta_\psi = 1 - \rho_\psi(\boldsymbol{b}, z, \boldsymbol{p}) = \int_{\boldsymbol{p}^2} d^2\boldsymbol{\kappa}\Phi(\boldsymbol{b}, x, \boldsymbol{\kappa}) \approx \frac{2\pi^2 T(\boldsymbol{b})\alpha_S(\boldsymbol{p}^2)}{N_c\boldsymbol{p}^2}\cdot\frac{\partial G(x, \boldsymbol{p}^2)}{\partial\log\boldsymbol{p}^2} = \frac{1}{2}\cdot\frac{Q_A^2(\boldsymbol{b})}{\boldsymbol{p}^2}\cdot\frac{\alpha_S(\boldsymbol{p}^2)}{\alpha_S(Q_A^2)G(x, Q_A^2)}\cdot\frac{\partial G(x, \boldsymbol{p}^2)}{\partial\log\boldsymbol{p}^2}. \quad (121)$$

It is important that δ_ψ is a manifestly positive valued quantity. It has a form similar to, but is numerically smaller than, the nuclear higher twist correction to $\phi(\boldsymbol{b}, x, \boldsymbol{\kappa})$.

In Fig. 12 we show the numerical results for the wave function distortion factor for the gold nucleus at several values of the optical thickness $\nu(\boldsymbol{b}) = \frac{1}{2}\sigma_0(x)T(\boldsymbol{b})$. At this point one needs to pay a due attention to an explicit dependence on the QCD running coupling $\alpha_S(r)$ on the small dipole-size r in Eq. (20). The discussion of its impact is found in [4,8], in the evaluation of the momentum spectra this running coupling must be taken at the largest relevant hard parameter, which in our case is $\boldsymbol{p}^2$. Correspondingly, in all the formulas for the dijet spectra, the dipole cross section for large dipoles $\sigma_0(x)$ must be understood as

$$\sigma_0(x) \Rightarrow \alpha_S(\boldsymbol{p}^2)\cdot\frac{4\pi^2}{N_c}\int\frac{d\kappa^2}{\kappa^4}\cdot\mathcal{F}(x,\kappa^2) = \alpha_S(\boldsymbol{p}^2)\sigma_0(x,\infty). \quad (122)$$

For this reason, the optical thickness of the nucleus $\nu(\boldsymbol{b})$ as a function of the impact parameter $\boldsymbol{b}$, shown in the left panel of Fig. 12, depends on the hard scale—the jet momentum. The wave function distortion factor $\rho_\psi(\boldsymbol{b}, z, \boldsymbol{p})$ is shown in the right panel of Fig. 12. The hard regime (121) for δ_ψ sets in at the momenta $p \gtrsim 1$ GeV. We reiterate that the saturated cross section $\sigma_0(x,\infty)$ is only an auxiliary parameter which does not enter directly the observable cross sections—the latter only depend on the saturation scale $Q_A^2(\boldsymbol{b})$, the discussion is found in Ref. [4].

In terms of the wave function distortion factor δ_ψ one readily finds

$$R_\psi(\boldsymbol{b},\boldsymbol{p},\Delta) = \frac{|\Psi(1;z,\boldsymbol{p}-\Delta)-\Psi(z,\boldsymbol{p}-z\Delta)|^2}{|\Psi(z,\boldsymbol{p}-\Delta)-\Psi(z,\boldsymbol{p}-z\Delta)|^2} = \frac{[(1-z)\Delta-\delta_\psi(\boldsymbol{p}-z\Delta)]^2}{(1-z)^2\Delta^2} = \frac{[(1-z)\Delta+\delta_\psi(\boldsymbol{p}_q-(1-z)\Delta)]^2}{(1-z)^2\Delta^2}. \quad (123)$$

The overall nuclear modification factor, the ratio of the nuclear, (114), and free-nucleon, (115), target contributions, is a product

$$R^{(3)}_{A/N}(\boldsymbol{b},\boldsymbol{p},\Delta) = R_g(\boldsymbol{b},\Delta)R_\psi(\boldsymbol{b},\boldsymbol{p},\Delta). \quad (124)$$

Here $R_g(\boldsymbol{b},\Delta)$ does not depend on the jet momentum $\boldsymbol{p}$ except for the weak dependence through $\alpha_S(\boldsymbol{p}^2)$. Evidently, $R_\psi(\boldsymbol{b},\boldsymbol{p},\Delta)$ is azimuthally asymmetric and favors Δ anticollinear to the gluon momentum and collinear to the quark momentum: in the back-to-back configuration, the gluon jet tends to have the transverse momentum smaller than the quark jet. The dominant contribution to the nuclear dijet cross section comes from $\Delta^2 \sim Q_A^2(\boldsymbol{b})$, and for hard dijets the asymmetry will be weak, of the order of $\sqrt{\delta_\psi} \sim Q_A(\boldsymbol{b})/p$.

Alternatively, if one keeps the quark transverse momentum fixed and increases the target mass number A, i.e., $Q_A^2(\boldsymbol{b})$ and δ_ψ thereof, the transverse momentum of the away gluon jet will decrease with A. The form of the $q \to qg$ splitting function favors production of the gluon jet at rapidities smaller than the quark jet. Then, the above correlation between the acoplanarity and quark momenta shall exhibit itself as a nuclear suppression of the away jet produced at rapidites smaller than the rapidity of the forward trigger jet. The numerical studies of this effect will be reported elsewhere.

C. Excitation of the sextet and 15-plet jets states

Here one must compare the contribution to the nuclear dijet spectrum (107) with its IA counterpart

$$\frac{T(\boldsymbol{b})d\sigma_N(\boldsymbol{p},\Delta)}{dzd^2\boldsymbol{p}d^2\Delta}\Big|_{6+15} = \frac{1}{2(2\pi)^2}T(\boldsymbol{b})f(\Delta)|\Psi(z,\boldsymbol{p}) - \Psi(z,\boldsymbol{p}-\Delta)|^2. \quad (125)$$

Note, that the nuclear cross section can be cast in the form reminiscent of a triple convolution

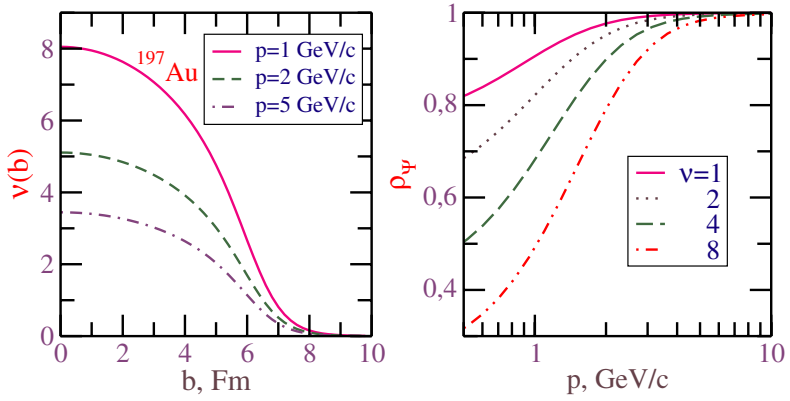

FIG. 12 (color online). The left panel shows the impact-parameter dependence of the optical thickness of the gold nucleus for several values of the gluon-jet momentum $\boldsymbol{p}$. The momentum dependence of the wave function distortion factor $\rho_\psi(\boldsymbol{b}, z, \boldsymbol{p})$ for several values of the optical thickness of the nucleus is presented in the right panel.

$$\frac{d\sigma_A(q^* \to qg)}{d^2\boldsymbol{b}dzd\boldsymbol{p}d\Delta}\Big|_{6+15} = T(\boldsymbol{b})\int_0^1 d\beta \int d^2\boldsymbol{\kappa}d^2\boldsymbol{\kappa}_1 d^2\boldsymbol{\kappa}_2 d^2\boldsymbol{\kappa}_3 \delta(\boldsymbol{\kappa}+\boldsymbol{\kappa}_1+\boldsymbol{\kappa}_2+\boldsymbol{\kappa}_3-\Delta)\times\Phi(1-\beta;\boldsymbol{b},\boldsymbol{\kappa}_1)$$
$$\times\Phi(C_2(1-\beta);\boldsymbol{b},\boldsymbol{\kappa}_2)\Phi(\beta;\boldsymbol{b},\boldsymbol{\kappa}_3)\frac{d\sigma_N(\beta;\boldsymbol{p}-\boldsymbol{\kappa}_1,\boldsymbol{\kappa})}{dzd^2(\boldsymbol{p}-\boldsymbol{\kappa}_1)d^2\boldsymbol{\kappa}}\Big|_{6+15}, \quad (126)$$

where $d\sigma_N(\beta;\boldsymbol{p})$ is the free-nucleon cross section calculated in terms of the ISI distorted wave functions. This convolution form suggests that at a fixed gluon-jet momentum $\boldsymbol{p}$, it will be a broader distribution of Δ than the free-nucleon cross section (for the related discussion see [4]).

The convolution property of $d\sigma_A$ is manifest for hard dijets, $\boldsymbol{p}^2 \gg \Delta^2, Q_A^2(\boldsymbol{b})$. Because the dominant contribution comes from $\boldsymbol{\kappa}_i^2 \lesssim Q_A^2(\boldsymbol{b})$, here one can neglect $\boldsymbol{\kappa}_{2,3}$ compared to $\boldsymbol{p}$, i.e., the nuclear distortion of the wave functions in $d\sigma_N(\beta;\boldsymbol{p})$, which then becomes independent of β. The result takes the form first found for DIS in [4]:

$$\frac{d\sigma_A(q^* \to qg)}{d^2\boldsymbol{b}dzd\boldsymbol{p}d\Delta}\Big|_{6+15} = T(\boldsymbol{b})\int_0^1 d\beta\int d^2\boldsymbol{\kappa}$$
$$\times\Phi(1+C_2(1-\beta);\boldsymbol{b},\Delta-\boldsymbol{\kappa})$$
$$\times\frac{d\sigma_N(\boldsymbol{p},\boldsymbol{\kappa})}{dzd^2\boldsymbol{p}d^2\boldsymbol{\kappa}}\Big|_{6+15}. \quad (127)$$

It is reminiscent of, but not identical to, the expectation from the simplistic reference scenario described in the Introduction—true, $\Phi(1+C_2(1-\beta);\boldsymbol{b},\Delta-\boldsymbol{\kappa})$ describes a convolution of incoherent ISI and FSI of participating partons, but the hard cross section $d\sigma_N$ is calculated in terms of the free nucleon, rather than collective nuclear, unintegrated glue.

The saturation scale for the distribution $\Phi(1+C_2(1-\beta);\boldsymbol{b},\Delta-\boldsymbol{\kappa})$ equals

$$Q_{A,\mathrm{eff}}^2 \approx [1+C_2(1-\beta)]Q_A^2(\boldsymbol{b}) \quad (128)$$

and the broadening of the acoplanarity distribution for the quark-gluon dijets is substantially stronger than that for the quark-antiquark dijets in DIS discussed in [4].

D. The fate of the dip for exactly back-to-back dijets

Nuclear effects partly smear out the dip of the dijet cross section at $\Delta = 0$ for exactly back-to-back quark-gluon dijets. First, the collective nuclear glue (97) is finite at $\Delta = 0$. Second, the contribution from color-triplet dijets is proportional to $|\Psi(1;z,\boldsymbol{p}-\Delta)-\Psi(z,\boldsymbol{p}-z\Delta)|^2$, which does not vanish at $\Delta = 0$, see Eq. (123). Third, a similar smearing of the dip at $\Delta = 0$ is obvious from the convolution form of the contribution from the sextet and 15-plet dijets: while the impulse approximation term (125) vanishes at $\Delta = 0$, the nuclear cross section (126) remains finite at $\Delta = 0$. The weakening of the dip at $\Delta = 0$ and of the double-hump azimuthal dependence of the dijet cross section for unequal momentum jets holds for nuclear targets too. The large-Δ collective nuclear glue (97) starts decreasing only at $\Delta^2 \gtrsim Q_A^2(\boldsymbol{b},x)$ and the double-hump structure will evidently spread with rising saturation scale $Q_A(\boldsymbol{b},x)$, which is a part of the above discussed generic azimuthal decorrelation of nuclear dijets, see also Ref. [4].

VII. MONOJETS FROM DIJETS: FRAGMENTATION VS GENUINE DIJETS

A. Monojets from dijets in the free-nucleon reactions

In the above discussion we implicitly assumed that the quark and gluon hard jets are separated by a large azimuthal angle and the acoplanarity momentum is small compared to the jet momenta $\Delta^2 \lesssim \boldsymbol{p}^2$, $(\boldsymbol{p}-\Delta)^2$. An interesting new situation is encountered when the quark and gluon jets start merging. Specifically, the wave function $\Psi(z,\boldsymbol{p}-z\Delta)$ which enters the color-triplet dijet cross section (115) has a pole when $\boldsymbol{p}-z\Delta = 0$, i.e., when the gluon and quark are collinear,

$$\boldsymbol{p} = z\Delta, \qquad \boldsymbol{p}_q = \Delta-\boldsymbol{p} = (1-z)\Delta = z_q\Delta. \quad (129)$$

In the vicinity of the pole the qg production cross section has the factorized form

$$\frac{d\sigma_N(q^* \to qg)}{dzd^2\boldsymbol{p}d^2\Delta}\Big|_{\mathrm{monojet}} = \frac{1}{2(2\pi)^2}f(\Delta)|\Psi(z,\boldsymbol{p}-z\Delta)|^2. \quad (130)$$

Now recall that $\Psi(z,\boldsymbol{p}-z\Delta)$ is precisely a probability amplitude to find the gluon with the momentum $\boldsymbol{k}_\perp = \boldsymbol{p}-z\Delta$ transversal with respect to the axis of the quark jet with the momentum Δ, and $|\Psi(z,\boldsymbol{p}-z\Delta)|^2$ of Eq. (88) is proportional to the familiar splitting function $P_{gq}(z)$, which is precisely the driving term of the quark-jet fragmentation function. Consequently, the contribution (130) must be treated as a fragmentation of the scattered quark into the quark and gluon, $q' \to qg$. The quark pole contribution will dominate if

$$\boldsymbol{k}_\perp^2 \ll (\boldsymbol{p}-\Delta)^2 = \boldsymbol{p}_q^2. \quad (131)$$

From the experimental point of view, the corresponding final state is a monojet of the transverse momentum Δ. The transverse momentum of such a monojet will be compensated by an away jet produced at midrapidity or the nucleus hemisphere of pA collisions.

In terms of Feynman diagrams of Fig. 2—for the free-nucleon target one takes the single-gluon exchange—the monojet production is a property of the diagram (c). Indeed, the cross section (130) is proportional to precisely the differential cross section of quasielastic scattering of

the projectile quark off the nucleon target—the latter is evidently proportional to the unintegrated gluon density of the target proton $f(\Delta)$. The two classes of Feynman diagrams in Fig. 2(b) and 2(c) are integral parts of the gauge-invariant description of the QCD Bremsstrahlung excitation of the qg state. Still, the isolation of the pole contribution from the gauge-invariant combinations

$$|\Psi(1; z, \boldsymbol{p} - \Delta) - \Psi(z, \boldsymbol{p} - z\Delta)|^2 = |\Psi(1; z, \boldsymbol{p}_q) - \Psi(z, \boldsymbol{p} - z\Delta)|^2$$

in (92), and of the monojet contribution to the generic dijet cross section would not conflict gauge invariance. In order to conform to the jet-finding algorithms, the production of the quark and gluon within the jet-defining cone must be treated as a fragmentation of the monojet; if the azimuthal angle between the quark and gluon is larger than the jet-defining angle, the two jets must be viewed as independent ones.

The monojet-pole contribution is absent in the excitation of the sextet and 15-plet final states. The combination of the wave functions, which enters Eq. (125),

$$|\Psi(z, \boldsymbol{p}) - \Psi(z, \boldsymbol{p} - \Delta)|^2 \propto \frac{(\boldsymbol{p} + \boldsymbol{p}_q)^2}{\boldsymbol{p}^2 \boldsymbol{p}_q^2},$$

is finite for all orientations of the quark and gluon jets.

The quark-tagged pQCD gluon Bremsstrahlung considered here is already the higher order process, the lowest order pQCD process in qN interaction is the radiationless quasielastic scattering of the quark. Naive application of fragmentation $q' \to qg$ to this lowest order process would evidently lead to a double counting, because the fragmentation is manifestly a monojet part of our dijet cross section. The integration over the gluon momentum $\boldsymbol{k}_\perp$ in the inclusive cross section would yield the familiar collinear logarithm, which must be reabsorbed into the definition of the fragmentation function at the starting scale. Simultaneously, one must include the virtual radiative correction to the radiationless quasielastic scattering of the incident quark off the target nucleon. The treatment of these virtual corrections to quasielastic scattering and elimination of double counting go beyond the scope of the present study and will be addressed elsewhere. We only want to comment that if one would insist on the description of monojets in terms of the fragmentation of the quark, then the interplay of the virtual correction to the radiationless quasielastic scattering and of the collinear logarithm in the monojet component of the dijet cross section may entail a departure of the fragmentation function from that defined in the e^+e^--annihilation.

B. Monojets from dijets off a nuclear target

The presence of the monojet pole (129) in the nuclear dijet cross section (107) is manifest:

$$\left.\frac{d\sigma_A(q^* \to qg)}{d^2\boldsymbol{b}dzd\boldsymbol{p}d\Delta}\right|_{\text{monojet}} = \frac{1}{2(2\pi)^2} T(\boldsymbol{b})\phi(\boldsymbol{b}, x, \Delta) \times |\Psi(z, \boldsymbol{p} - z\Delta)|^2. \quad (132)$$

It factorizes precisely as the free-nucleon cross section: the differential cross section of quasielastic quark-nucleus scattering, proportional to the unintegrated collective gluon density of the nucleus, times the fragmentation of the scattered quark to the gluon and quark given by $|\Psi(z, \boldsymbol{p} - z\Delta)|^2$, which does not depend on the target. However, the virtual radiative correction to the radiationless quasielastic scattering of the incident quark off the target nucleus and the elimination of double counting are likely to depend on the acoplanarity momentum Δ and the shape of the collective nuclear glue $\phi(\boldsymbol{b}, x, \Delta)$. Should this be the case, such a dependence could be reinterpreted as a nuclear modification of the fragmentation function; this issue will be addressed elsewhere.

As it was the case for the free-nucleon target, excitation of the sextet and 15-plet final states is free of the monojet singularities. To be more precise, the wave function singularities in the integrand of the sextet and 15-plet contribution to (107) occur in the intermediate state, at $\boldsymbol{p} - \boldsymbol{\kappa}_1 - \boldsymbol{\kappa} = 0$ and $\boldsymbol{p} - \boldsymbol{\kappa}_1 = 0$. However, they are integrated out in the observed dijet cross section. It is still instructive to look at the effect of these singularities in the monojet kinematics $\Delta^2 \gg \boldsymbol{p}^2 \gtrsim Q_A^2(\boldsymbol{b})$.

Consider first the contribution from the intermediate pole at $\boldsymbol{p} - \boldsymbol{\kappa}_1 = 0$. The relevant $\boldsymbol{\kappa}_i$ integrations are of the form

$$\begin{aligned}&\int d^2\boldsymbol{\kappa}_1 d^2\boldsymbol{\kappa} f(x, \boldsymbol{\kappa})\Phi(1 - \beta, \boldsymbol{b}, x, \Delta - \boldsymbol{\kappa}_1 - \boldsymbol{\kappa}) \\ &\quad \times \Phi(\beta + C_2(1 - \beta), \boldsymbol{b}, x, \boldsymbol{\kappa}_1) \times |\Psi(\beta; z, \boldsymbol{p} - \boldsymbol{\kappa}_1)|^2 \\ &= \Phi(\beta + C_2(1 - \beta); \boldsymbol{b}, x, \boldsymbol{p}) \int^{p^2} d^2\boldsymbol{k} |\Psi(\beta; z, \boldsymbol{k})|^2 \\ &\quad \times \int d^2\boldsymbol{\kappa} f(x, \boldsymbol{\kappa})\Phi(1 - \beta, \boldsymbol{b}, x, \Delta - \boldsymbol{p} - \boldsymbol{\kappa}). \quad (133)\end{aligned}$$

For the considered hard jets

$$\Phi(1 - \beta, \boldsymbol{b}, x, \Delta - \boldsymbol{p} - \boldsymbol{\kappa}) = \frac{1}{2}(1 - \beta)T(\boldsymbol{b})f(\Delta - \boldsymbol{p} - \boldsymbol{\kappa}) \quad (134)$$

and the convolution in (133) equals [4,8]

$$\int d^2\boldsymbol{\kappa} f(x, \boldsymbol{\kappa})\Phi(1 - \beta, \boldsymbol{b}, x, \Delta - \boldsymbol{p} - \boldsymbol{\kappa}) = (1 - \beta)T(\boldsymbol{b})f(\Delta - \boldsymbol{p}). \quad (135)$$

The resulting contribution from the intermediate pole of the wave function at $\boldsymbol{p} - \boldsymbol{\kappa}_1 = 0$ is proportional to

$$T^2(\boldsymbol{b})f(\Delta - \boldsymbol{p})f(\boldsymbol{p})P_{gq}(z) = T^2(\boldsymbol{b})f(\boldsymbol{p}_g)f(\boldsymbol{p}_q)P_{gq}(z) \quad (136)$$

and has the form of the product of the differential cross sections of independent quasielastic scattering of the quark and gluon fragments of the incident quark. It does not depend on the azimuthal angle between the quark and gluon jets at all, and has no collinear singularity. A similar situation has been found to occur in our previous study of the production of hard quark-antiquark dijets in πA collisions [13]. The contribution from the pole at $\boldsymbol{p} - \boldsymbol{\kappa}_1 - \boldsymbol{\kappa} = 0$ is entirely similar.

IX. CONCLUSIONS

The prime task of the pQCD theory of nuclear interactions is to establish a link between observables for different hard processes in a nuclear environment, as close to familiar linear $k_\perp$ factorization for high-energy interactions on the free-nucleon target as possible. The reported derivation of nuclear modifications of the quark-gluon production in quark-nucleus collisions is a major step towards this goal. Our principal result—the nonlinear $k_\perp$-factorization relation (107)—gives one observable—the spectrum of quark-gluon dijets produced off a nuclear target—as a quadrature in terms of the collective nuclear unintegrated glue defined by another observable—the amplitude of coherent diffractive dijet production off nuclei. Furthermore, precisely the same collective nuclear glue furnishes linear $k_\perp$ factorization for leading single-quark jet spectrum in DIS off nuclei and nonlinear $k_\perp$ factorization for single-jet spectra from other pQCD subprocesses in a nuclear environment.

The derived quark-gluon dijet cross section can be decomposed into three major contributions. The excitation of qg dijets in higher-sextet and 15-plet color representations gives rise to the sixth order nonlinearity in gluon densities, compared to the fifth order nonlinearity for $q\bar{q}$ dijets in DIS. A part of the nonlinearity comes from the free-nucleon gluon density which emerges in all instances of excitation of higher color representations (see also the related discussion of the $1/(N_c^2 - 1)$ expansion in Ref. [4]). The matrix elements of transitions from lower to higher color representations are suppressed at large N_c, but this suppression is compensated for by the large number of states in higher representations. The coherent diffraction, in which the final dipole is produced in exactly the same color state as the incident quark, is not suppressed by large N_c, but because of the color-nonsinglet incident partons the diffractive contribution is suppressed by an overall nuclear attenuation and will only come from collisions at the diffuse edge of a nucleus. A new feature of qA collisions in contrast to DIS is inelastic production of qg states in the same color representation as the incident parton. Such color rotations within the same representation are not suppressed at large N_c. This contribution has the form which superficially looks like satisfying the linear $k_\perp$ factorization in terms of the collective nuclear gluon density. However, it contains the nuclear-distorted wave function of the qg Fock state and, consequently, is a cubic functional of the collective nuclear glue.

The above three components of the quark-gluon dijet cross section differ by more than the degree of the nonlinearity. The coherent diffractive mechanism and the excitation of quark-gluon dijets in the same color representation as the incident quark are explicitly calculable in terms of the collective nuclear glue of Eq. (94) which is defined for the whole nucleus. This is not the case for the excitation of quark-gluon dijets in higher color multiplets. It is proportional to the unintegrated gluon density in the free nucleon. The coherent initial-state interaction, before the excitation of higher color multiplets at the depth β of the nucleus, must be described in terms of the unintegrated collective glue (100) defined for the slice β of the nucleus.

The quantum mechanical coherence properties of our final result are highly nontrivial: coherent distortions of the qg wave function are complemented by incoherent broadening of the incident quark transverse momentum distribution in the same slice $[0, \beta]$ of the nucleus. Likewise, the final-state interactions after the excitation of higher multiplets must be described in terms of the unintegrated collective glue defined for the slice $(1 - \beta)$ of the nucleus. Furthermore, besides the collective nuclear glue defined for color-singlet quark-antiquark dipole, there emerges a new nuclear gluon density which depends on the Casimir operators of higher quark-gluon color representations, i.e., the gluon field of the nucleus must be described by a density matrix in the space of color representations.

A comparison of the results for the quark-gluon dijets in quark-nucleon collisions to the excitation of quark-antiquark dijets in DIS and gluon-nucleus collisions reveals a vast variety of nonlinear quadratures in terms of the collective nuclear glue. We have shown how, depending on the color properties of the relevant pQCD subprocesses, different results fall into four universality classes for nonlinear $k_\perp$ factorization. A tempting simplistic scenario for hard processes in a nuclear matter as a hard scattering of the incident parton off the collective nuclear glue preceded and followed by incoherent soft initial and final-state interactions is borne out by none of our universality classes.

The central technical point of our derivation is the β-unintegrated form of the dijet cross section. Only this form makes manifest the nonlinear $k_\perp$ factorization for the dijet observables in terms of another physics observable—the coherent diffractive dijet amplitude. Precisely because of this unifying aspect and the establishment of the universality classes we regard our results as nonlinear $k_\perp$-factorization theorems for dijet production in a nuclear environment. We reiterate that the β-dependence of integrands of the dijet cross section is not an artifact of our formalism, rather it emphasizes nontrivial non-Abelian properties of the intranuclear evolution of color dipoles, different color properties of the initial-state and final-state

interactions, the necessity of the color density matrix description of the collective nuclear glue and nontrivial interplay of coherent and incoherent distortions. The collective nuclear glue (100) defined for different slices of the nucleus emerges as an indispensable entity of nonlinear $k_\perp$ factorization and is at the heart of the identification of universality classes of nonlinear $k_\perp$ factorization. The direct multidimensional Fourier transform of the Sylvester expansion (82), the numerator of which can be presented in terms of the gluon density defined for the whole nucleus or classical field, like e.g. the color glass condensate approach [36], is technically possible. Such a brute force numerical calculation would obscure the above described ISI/FSI interpretation of the dijet cross section and miss the nonlinear $k_\perp$ factorization which furnishes the unified description of different hard processes.

The representation for the dijet cross section similar to our master formula (13) has been discussed recently by several authors [10–12], but these works stopped short of the solution of the coupled-channel intranuclear evolution for the 4-parton state. Although major ingredients for the diagonalization of the four-body S-matrix are found in our earlier work on dijets in DIS [4], the case of the qg dijets has its own tricky points. For this reason, we felt it imperative to present full technical details of this diagonalization.

The emphasis of the present communication was on the formalism, the numerical applications will be reported elsewhere. The nuclear coherency condition, $x \lesssim x_A \approx 0.1 \cdot A^{-1/3}$, restricts the applicability domain of our formalism to the forward part of the proton hemisphere of pA collisions at RHIC. Although the required coherency condition does not hold for the midrapidity dijets studied so far at RHIC [37], our predictions could be tested after the detectors at RHIC II will be upgraded to cover the proton fragmentation region [19].

ACKNOWLEDGMENTS

We are grateful to the referee for useful suggestions on the presentation. This work was partly supported by Grant No. DFG 436 RUS 17/101/04.

Note added.—Recently an e-print by Baier *et al.* on a related discussion of dijet production has been posted [38]. The reported numerical results on azimuthal correlations of back-to-back dijets and the dip at $\Delta = 0$ are based on the direct numerical Fourier transform of the Sylvester expansion in the color-dipole master formula for the dijet spectrum. The observed trends are in line with our brief discussion in Sec. VII D which we added to clarify the relationship between the two approaches.

[1] E. Leader and E. Predazzi, *Introduction to Gauge Theories and Modern Particle Physics*, Vols. 1 & 2 (Cambridge University Press, Cambridge, England, 1996); G. Sterman, *An Introduction to Quantum Field Theory* (Cambridge University Press, Cambridge, England, 1993); R. K. Ellis, W. J. Stirling, and B. R. Webber, Cambridge Monogr. Part. Phys., Nucl. Phys., Cosmol. **8**, 1 (1996).

[2] N. N. Nikolaev and V. I. Zakharov, Yad. Fiz. **21**, 434 (1975) [Sov. J. Nucl. Phys. **21**, 227 (1975)]; Phys. Lett. B **55**, 397 (1975).

[3] I. P. Ivanov, N. N. Nikolaev, W. Schäfer, B. G. Zakharov, and V. R. Zoller, Lectures on Diffraction and Saturation of Nuclear Partons in DIS off heavy Nuclei, Proceedings of 36th Annual Winter School on Nuclear and Particle Physics (PINP 2002) and 8th St. Petersburg School on Theoretical Physics, St. Petersburg, Russia, 2002 (unpublished).

[4] N. N. Nikolaev, W. Schäfer, B. G. Zakharov, and V. R. Zoller, Zh. Eksp. Teor. Fiz. **124**, 491 (2003) [J. Exp. Theor. Phys. **97**, 441 (2003).

[5] N. N. Nikolaev, W. Schäfer, B. G. Zakharov, and V. R. Zoller, ''Strbske Pleso 2004, Deep inelastic scattering,'' in Proceedings of 12th International Workshop on Deep Inelastic Scattering (DIS 2004), Strbske Pleso, Slovakia, 2004, edited by D. Bruncko, J. Ferencei, and P. Strizenec, p. 413 (unpublished).

[6] N. N. Nikolaev and W. Schäfer, Phys. Rev. D **71**, 014023 (2005).

[7] N. N. Nikolaev and B. G. Zakharov, Phys. Lett. B **332**, 177 (1994).

[8] N. N. Nikolaev, W. Schäfer, and G. Schwiete, Phys. Rev. D **63**, 014020 (2001).

[9] B. Andersson *et al.* (Small x Collaboration), Eur. Phys. J. C **25**, 77 (2002); J. R. Andersen *et al.* (Small x Collaboration), Eur. Phys. J. C **35**, 67 (2004).

[10] J. P. Blaizot, F. Gelis, and R. Venugopalan, Nucl. Phys. **A743**, 57 (2004).

[11] J. Jalilian-Marian and Y. V. Kovchegov, Phys. Rev. D **70**, 114017 (2004).

[12] R. Venugopalan, hep-ph/0502190; H. Fujii, F. Gelis, and R. Venugopalan, hep-ph/0502204.

[13] N. N. Nikolaev, W. Schäfer, B. G. Zakharov, and V. R. Zoller, Yad. Fiz. **68**, 692 (2005) [Phys. At. Nucl. **68**, 661 (2005)].

[14] B. G. Zakharov, Yad. Fiz. **46**, 148 (1987) [Sov. J. Nucl. Phys. **46**, 92 (1987)].

[15] N. N. Nikolaev, G. Piller, and B. G. Zakharov, Zh. Eksp. Teor. Fiz. **108**, 1554 (1995) [J. Exp. Theor. Phys. **81**, 851 (1995); Z. Phys. A **354**, 99 (1996).

[16] N. N. Nikolaev and B. G. Zakharov, Z. Phys. C **49**, 607 (1991).

[17] N. N. Nikolaev and B. G. Zakharov, Zh. Eksp. Teor. Fiz.

105, 1117 (1994) [J. Exp. Theor. Phys. **78**, 598 (1994)]; N. N. Nikolaev and B. G. Zakharov, Z. Phys. C **64**, 631 (1994).

[18] N. N. Nikolaev, W. Schäfer, and B. G. Zakharov, hep-ph/0502018.

[19] L. C. Bland *et al.*, hep-ex/0502040; P. Steinberg *et al.*, nucl-ex/0503002.

[20] V. Barone, M. Genovese, N. N. Nikolaev, E. Predazzi, and B. G. Zakharov, Z. Phys. C **58**, 541 (1993).

[21] N. N. Nikolaev and B. G. Zakharov, Z. Phys. C **53**, 331 (1992).

[22] B. G. Zakharov, JETP Lett. **63**, 952 (1996); JETP Lett. **65**, 615 (1997); Yad. Fiz. **61**, 924 (1998) [Phys. At. Nucl. **61**, 838 (1998); R. Baier, D. Schiff, and B. G. Zakharov, Annu. Rev. Nucl. Part. Sci. **50**, 37 (2000).

[23] N. N. Nikolaev and B. G. Zakharov, Phys. Lett. B **332**, 184 (1994).

[24] N. N. Nikolaev, B. G. Zakharov, and V. R. Zoller, JETP Lett. **59**, 6 (1994).

[25] E. A. Kuraev, L. N. Lipatov, and V. S. Fadin, Zh. Eksp. Teor. Fiz. **72**, 377 (1977) [Sov. Phys. JETP **45**, 199 (1977)]; I. I. Balitsky and L. N. Lipatov, Yad. Fiz. **28**, 1597 (1978) [Sov. J. Nucl. Phys. **28**, 822 (1978)].

[26] R. J. Glauber, *Lectures in Theoretical Physics*, edited by W. E. Brittin *et al.* (Interscience, New York, 1959), Vol. 1, p. 315.

[27] V. N. Gribov, Zh. Eksp. Teor. Fiz. **56**, 892 (1969) [Sov. Phys. JETP **29**, 483 (1969)].

[28] P. Cvitanović, Group Theory, Webbook version 8.3.7, http://www.nbi.dk/GroupTheory/.

[29] I. P. Ivanov and N. N. Nikolaev, Phys. Rev. D **65**, 054004 (2002); Yad. Fiz. **64**, 813 (2001) [Phys. At. Nucl. **64**, 753 (2001)].

[30] N. N. Nikolaev, W. Schäfer, and G. Schwiete, Pis'ma Zh. Eksp. Teor. Fiz. **72**, 583 (2000) [JETP Lett. **72**, 405 (2000)].

[31] N. N. Nikolaev, W. Schäfer, B. G. Zakharov, and V. R. Zoller, Pis'ma Zh. Eksp. Teor. Fiz. **76**, 231 (2002) [JETP Lett. **76**, 195 (2002)].

[32] N. N. Nikolaev, B. G. Zakharov, and V. R. Zoller, Z. Phys. A **351**, 435 (1995).

[33] T. Sjostrand and V. A. Khoze, Z. Phys. C **62**, 281 (1994).

[34] T. Sjostrand, L. Lonnblad, S. Mrenna, and P. Skands, hep-ph/0308153; G. Abbiendi *et al.* (OPAL Collaboration), Eur. Phys. J. C **36**, 297 (2004); R. Strohmer, Int. J. Mod. Phys. A **18**, 5127 (2003).

[35] M. Derrick *et al.* (ZEUS Collaboration), Phys. Lett. B **315**, 481 (1993); T. Ahmed *et al.* (H1 Collaboration), Nucl. Phys. **B429**, 477 (1994); S. Chekanov *et al.* (ZEUS Collaboration), Nucl. Phys. **B713**, 3 (2005).

[36] L. D. McLerran and R. Venugopalan, Phys. Rev. D **49**, 2233 (1994); J. Jalilian-Marian, A. Kovner, L. D. McLerran, and H. Weigert, Phys. Rev. D **55**, 5414 (1997); A. H. Mueller, in *Proceedings of QCD Perspectives on Hot and Dense Matter, Cargese, France, 2001*, edited by J.-P. Blaizot and E. Iancu (Kluwer, Dordrecht, 2002); E. Iancu, A. Leonidov, and L. McLerran, in *Proceedings of QCD Perspectives on Hot and Dense Matter, Cargese, France, 2001* edited by J.-P. Blaizot and E. Iancu (Kluwer, Dordrecht, 2002); E. Iancu and R. Venugopalan, in *Quark Gluon Plasma 3,*, edited by R. C. Hwa and X. N. Wang (World Scientific, Singapore, 2004).

[37] C. Adler *et al.* (STAR Collaboration), Phys. Rev. Lett. **90**, 082302 (2003).

[38] R. Baier, A. Kovner, M. Nardi, and U. A. Wiedemann, hep-ph/0506126.